NASA-TM-79026 19790008473

NASA Technical Memorandum 79026

THREE-DIMENSIONAL FINITE-ELEMENT ELASTIC ANALYSIS OF A THERMALLY CYCLED SINGLE-EDGE WEDGE GEOMETRY SPECIMEN

Peter T. Bizon, Richard J. Hill, Bruce P. Guilliams,
Sandra K. Drake, and Jeffrey L. Kladden
Lewis Research Center
Cleveland, Ohio

January 1979

1 Report No	2 Government Accession No	3 Recipient's Catalog No
NASA TM-79026		

4 Title and Subtitle	5 Report Date
THREE-DIMENSIONAL FINITE-ELEMENT ELASTIC ANALYSIS OF A THERMALLY CYCLED SINGLE-EDGE WEDGE GEOMETRY SPECIMEN	6 Performing Organization Code

7 Author(s)	8 Performing Organization Report No
Peter T Bizon*, Richard J Hill**, Bruce P Gulliams*, Sandra K Drake**, and Jeffrey L Kladden**	E-9861
	10 Work Unit No

9 Performing Organization Name and Address	11 Contract or Grant No
National Aeronautics and Space Administration Lewis Research Center Cleveland, Ohio 44135	
	13 Type of Report and Period Covered
12 Sponsoring Agency Name and Address	Technical Memorandum
National Aeronautics and Space Administration Washington, D C 20546	14 Sponsoring Agency Code

15 Supplementary Notes

*Lewis Research Center, Cleveland, Ohio

**Air Force Aero Propulsion Laboratory, Wright-Patterson Air Force Base, Ohio

16 Abstract

An elastic stress analysis was performed on a wedge specimen (prismatic bar with single-wedge cross section) subjected to thermal cycles in fluidized beds Seven different combinations consisting of three alloys (NASA TAZ-8A, 316 stainless steel, and A-286) and four thermal cycling conditions were analyzed The analyses were performed as a joint effort of two laboratories using different models and computer programs (NASTRAN and ISO3DQ) Stress, strain, and temperature results are presented

17 Key Words (Suggested by Author(s))	18 Distribution Statement
Finite element, Elastic deformation, Computer programs, Thermal fatigue, Fluidized bed, Stress analysis, Thermal stresses, Structural analysis	Unclassified - unlimited STAR Category 39

19 Security Classif (of this report)	20 Security Classif (of this page)	21 No of Pages	22 Price*
Unclassified	Unclassified		

* For sale by the National Technical Information Service Springfield Virginia 22161

THREE-DIMENSIONAL FINITE-ELEMENT ELASTIC ANALYSIS OF A THERMALLY CYCLED SINGLE-EDGE WEDGE GEOMETRY SPECIMEN

by Peter T. Bizon*, Richard J. Hill**, Bruce P. Guilliams*, Sandra K. Drake**, and Jeffrey L. Kladden**

*National Aeronautics and Space Administration
Lewis Research Center
Cleveland, Ohio

**Air Force Aero Propulsion Laboratory
Wright-Patterson Air Force Base, Ohio

E-9861

SUMMARY

Conventional three-dimensional finite-element elastic analysis techniques were used to analyze a single-edge wedge geometry specimen thermally cycled in fluidized beds. This analysis was performed as a joint program of the Lewis Research Center of NASA and the Air Force Aero Propulsion Laboratory (AFAPL). Lewis used a general structural analysis program (NASTRAN) with a fine mesh to analyze a severe heating time increment of one alloy. The AFAPL used a specialized blade and disk program (ISO3DQ) and a coarse mesh for the same time increment and alloy. Comparison of results for this combination using both methods showed very good agreement. The remaining combinations of test conditions and alloys considered were then analyzed using the coarse mesh model with the ISO3DQ computer program.

Seven different combinations of alloys and cycling conditions were analyzed using specimens of identical geometry. The alloys were NASA TAZ-8A, 316 stainless steel, and A-286. The cycling condition for the first mentioned alloy was alternate 3-minute immersions in beds maintained at 316° and 1088° C (600° and 1990° F). Cycling conditions for each of the other two alloys were alternate 4-minute immersions in a cooling bed always maintained at 21° C (70° F) and a heating bed maintained at 740°, 850°, or 960° C (1364°, 1562°, or 1760° F). The test conditions selected were those that would result in reasonable failure times for the alloys. The most severe testing condition was used for the high-temperature alloy (NASA TAZ-8A) with less severe conditions used for the other two intermediate-temperature alloys.

The temperature, strain and stress at the critical location for a typical cycle are presented herein for each of the seven combinations analyzed. In addition, the temperature, strain and stress distributions over the complete wedge are given at the time of both maximum and minimum longitudinal leading-edge strain. The maximum longitudinal strainrange (algebraic difference between maximum and minimum longitudinal strain) varied from 0.35 to 0.56 percent strain.

INTRODUCTION

One important area of research in advancing the technology of aircraft gas turbine engines is to provide an accurate assessment of the life prediction procedures for blades and vanes of gas turbine engines. In order to further develop and evaluate life prediction methods, simulated hardware components are tested in the laboratory using carefully controlled conditions. Comparison of the experimentally measured life to that which is analytically predicted is used as a means of evaluating life prediction theories.

One experimental laboratory method for measuring thermal fatigue life is the cycling of wedge specimens in fluidized beds. Such tests can provide life data as well as transient temperature data that is obtained under carefully controlled conditions. Reference 1 contains a compilation of such data including a description of the facility and test procedure. References 2-9 contain incremental portions of such data relative to the evaluations described in this paper.

Two fluidized beds were used for rapidly heating and cooling specimens in the form of prismatic bars with single-wedge constant cross-sections. These specimens failed by thermal fatigue cracking which is usually the predominant failure mode of aircraft engine first stage turbine blades and vanes. Thermal fatigue is defined as the cracking of a material caused by repeated temperature changes which induce cyclic stresses and strains.

The turbine component life prediction methods currently being studied at Lewis are discussed in references 10-15. To predict specimen thermal fatigue life (defined as time-to-cracking) for the fluidized bed tests, it is necessary to know the stress/strain-temperature-time history at the crack initiation site

The objective of this investigation was to analytically determine the elastic stress/strain-temperature-time history at the critical location for a single-edge wedge geometry specimen cycled in fluidized beds. This was performed as a joint program between NASA and the Air Force and utilized three-dimensional finite-element elastic analysis techniques. Lewis used the NASTRAN computer program while the Air Force Aero Propulsion Laboratory (AFAPL) used the ISO3DQ program.

Seven combinations consisting of three alloys and four different cycling conditions were analyzed. NASA TAZ-8A alloy was analyzed for the condition involving cycling in fluidized beds maintained at 316° and 1088° C (600° and 1990° F), with the immersion time in each bed being 3 minutes. Alloys 316 stainless steel and A-286 were each analyzed for three different cyclic conditions. The heating bed for the three conditions was 740°, 850°, or 960° C (1364°, 1562°, or 1760° F). The cooling bed was always 21° C (70° F). Immersion time in both hot and cold beds was 4 minutes. The cycling test conditions were those that resulted in thermal fatigue cracking in a reasonable number of cycles. The most severe testing condition was used for the high temperature alloy (NASA TAZ-8A) with less severe cycling conditions used for the other two intermediate temperature alloys.

Due to symmetry, a discretized model of only a quarter of the wedge specimen was necessary for analysis. First a model with a fine mesh for a severe condition was analyzed using the NASTRAN program. Then a model with various coarse meshes for the same condition were analyzed using the ISO3DQ computer program. A coarse mesh model for the ISO3DQ analysis was selected which gave essentially the same results as using the fine mesh model with the NASTRAN analysis. The remaining combinations were then analyzed using the coarse mesh model and ISO3DQ program. Such analyses provide the strainrange and stress/strain-temperature-time history so important for evaluation of life prediction theories such as strainrange partitioning.

This work was conducted in the U.S. customary system of units. Conversion to International System of Units (SI) was made for reporting purposes only.

INPUT FOR COMPUTER PROGRAMS

The alloys and test conditions for the seven combinations are given in table I. The necessary inputs to perform the analyses were: (1) the geometry of the single-edge wedge, (2) the elastic and physical material properties of the three alloys, and (3) a complete temperature distribution at various times throughout the cycle This section gives a detailed description of these inputs.

Wedge Geometry

The geometry for the single-edge wedge is shown in figure 1(a) The computer plots of the models used for analysis as well as a typical element are shown in figure 1(b) for the NASTRAN program and in figure 1(c) for the ISO3DQ program The model for both programs "squared-off" the leading-edge radius to a 1 02 mm (0.040 in.) length. Otherwise the models duplicated the geometry of the wedge exactly. Detail discussion of the modeling is given in the section Description of Analyses.

Alloy Properties

The temperature independent and temperature dependent alloy properties used for the elastic analyses are given in tables II and III respectively. The properties required for the analyses were Poisson's ratio, modulus of elasticity, and the mean coefficient of thermal expansion. The programs required a value for density to obtain results (zero mass elements were not permitted) although the results are independent of density. The properties for all alloys except the mean coefficient of thermal expansion for NASA TAZ-8A alloy were obtained from references 16 and 17. The mean coefficient of thermal expansion for NASA TAZ-8A alloy was independently determined and is reported here for the first time. This, as well as all data in reference 16, was determined from the same heat used for fabricating the single-edge wedge test and calibration specimens.

Temperature Loading

The transient temperature loading on the single-edge wedges was determined from thermocouple data. Calibration specimens of the three alloys were instrumented chordwise at the midspan with five embedded thermocouples and cycled in the fluidized beds (schematically shown in figure 2). The location of the thermocouples at the wedge cross section is shown in figure 3. The Inconel 600 sheathed thermocouples were mounted in grooves milled in the surface of the specimen and secured by a ceramic cement. The grooves were 0.56 mm (0.022 in.) wide and 0.5 mm (0.02 in.) deep. Other details of the installation and procedure are given in reference 1. The thermocouple outputs were cross-plotted to give temperatures of the midchord at the midspan at various time increments after immersion into the fluidized beds. These data are presented as figure 3 for the seven combinations analyzed. It was assumed that there was no temperature gradient through the thickness of the wedge.

Another set of thermocouple data was taken with five thermocouples mounted along the leading edge over half the span. These data revealed a longitudinal (along the span of the blade) temperature gradient which varied with the different time increments. The maximum variation was about 16 percent greater at the ends of the wedge compared to the midspan and occurred after 30 seconds of heating. However, for any one time increment it was found that the ratio of the leading edge midspan temperature to that of any other span location was nominally the same for the seven investigated combinations. A least squares best fit parabola was determined for each time increment and this is presented in table IV. This parabolic temperature variation along the span was assumed over the complete chord of the wedge.

The temperatures at midspan were determined from the appropriate plot in figure 3. For locations other than midspan, the temperatures were determined by using the midspan temperature modified by the values given in table IV. Therefore, by use of figure 3 and table IV the temperature distribution at any point of the wedge was determined.

DESCRIPTION OF ANALYSES

Both computer programs used three-dimensional finite-element procedures to obtain an elastic analysis of the single-edge wedge geometry specimen. The NASTRAN program was used to obtain an analysis only for NASA TAZ-8A alloy for the time increment 15 seconds after immersion into the heating bed. The ISO3DQ analysis, for the combination involving a 3 minute immersion time (figure 3(a)), was performed at all 17 heating and cooling time increments. These results showed that after 90 seconds immersion, the rate of change of stresses and strains was reduced to a point where coarser time increments might be used without loss of accuracy. Therefore, for the other six combinations which involved an additional minute of immersion time, the analysis was performed at a total of only 16 heating and cooling time increments - not using the 105, 135, 165, 195, and 225 second time increments.

The NASTRAN program was developed by NASA for elastic analysis of generalized structures. The ISO3DQ program was developed under contract by the Air Force for elastic analysis - specifically aircraft gas turbine blades, vanes, and disks. Documentation of the NASTRAN program includes a theoretical manual (ref. 18), a programmer's manual (ref. 19), a user's manual (ref. 20), and a demonstration problem manual (ref. 21). Documentation of the ISO3DQ program includes a descriptive report (ref. 22) and a user's manual (ref. 23). For general information on the programs the reader is referred to these manuals. Specific information on how the wedge was modeled and analyzed using these programs is presented in the following sections

NASTRAN Computer Program

The model for the single-edge wedge was one-fourth of the structure as shown in figure 1(b). There are reflective planes of symmetry at the midchord and midspan for this structure. The nodal constraints on this model (using the axis notation given in fig. 1(b)) are as follows

1. No z-displacement for nodes on the midspan plane because of reflective symmetry.

2. No -displacement for nodes on the midchord plane because of reflective symmetry.

3. No x-displacement for the two nodes at the trailing edge of the midspan plane to obtain a reference for displacements.

A fine mesh was used in the NASTRAN analysis so that it might be used as the "baseline" for comparison. The model consisted of 464 nodes for the 192 CHEXA2 (hexahedral) elements. A typical element is shown in figure 1(b). The discretization, including element and nodal identification, was done by hand - no mesh generator was used. The geometry was entered into the computer program by listing the coordinates of each node point from the origin shown in figure 1(b) Elements were selected so that the maximum aspect ratio for any element was always less than 2.5.

The complete table of temperature dependent properties (modulus of elasticity and mean coefficient of thermal expansion) for NASA TAZ-8A alloy was entered with 56^{o} C (100^{o} F) increments as given in table III. The program selected the value for these properties for each element by using the element temperature to linearly interpolate within this table. Since temperatures were assigned to nodes rather than elements, the element temperature was determined by the program by averaging the eight nodal temperatures. Since NASTRAN does not have the capability to input temperatures by use of equations, all temperatures were first hand calculated (using fig. 3(a) and table IV) and then entered for each node point.

The output selected from the NASTRAN program were the displacements, single point constraint forces, and stresses. The displacements and forces were given at the node points and the stresses were given at the element centroids. Stresses at the leading and trailing edges were obtained by extrapolation of plots through the centroids of the elements.

This program was run using level 16.0 of NASTRAN on a Univac 1110 computer. The plot given in figure 1(b) was done on a Calcomp plotter using the NASTRAN plot subroutine.

ISO3DQ Computer Program

The model for the ISO3DQ analysis was similar to that used for the NASTRAN program. One-fourth of the single-edge wedge was used considering midchord and midspan planes of symmetry as shown in figure 1(c). The nodal constraints were

identical to those used in the NASTRAN program so that a valid comparison could be made. The coarse mesh model selected consisted of 126 nodes for the 24 isoparametric elements. A typical element is shown in figure 1(c). The elements had midpoint nodes along the x-direction but not the y- and z-directions so that each element consisted of twelve nodes. The discretization, including element and nodal identification, was done using a mesh generator. This preprocessor (MESH3) is part of the ISO3DQ family of programs. This program required only the cross-section geometry of the wedge and some mesh parameters for the geometry input. The maximum aspect ratio for the elements was less than 17.

Values for the two temperature dependent properties (modulus of elasticity and mean coefficient of thermal expansion) were entered into the program as segments of table III. This table gives the modulus of elasticity and mean coefficient of thermal expansion for each alloy at 56^{o} C (100^{o} F) temperature increments. Six of a program limit of eight values of modulus and thermal coefficient for six given temperature increments (table III) were put into the program. The program selected the value for the two temperature dependent properties for each node by using the nodal temperature to linearly interpolate within the table.

The temperature loading was entered by means of a temperature table of eight chord temperatures at four different span locations. The program assigned a temperature to each node by weighted interpolation. Because temperatures were assigned to nodes rather than elements, a straight line gradient between adjacent nodes was assumed.

The output selected from the ISO3DQ program were the displacements, strains, and stresses. All of these values were determined at the node points. This set of data was put on tape for use by another program called PROUT3. The latter program, part of the ISO3DQ family, allows the amount and format of the output to be varied without requiring the complete program to be rerun. Both the MESH3 (preprocessor) and PROUT3 programs have plot capability

The ISO3DQ family of programs were run on the Wright-Patterson Air Force Base CDC 6600 computer. Plots (including figure 1(c)) were done using a Calcomp on-line plotter.

RESULTS AND DISCUSSION

The results are presented and discussed in three parts. First, comparison of the NASTRAN and ISO3DQ analyses for the check case are presented. Second, results for all seven combinations calculated by the ISO3DQ program are presented at the critical location. The critical location was taken as that point on the blade which had the maximum longitudinal strainrange (algebraic difference between maximum and minimum longitudinal strain) throughout the complete heating and cooling cycle. This location was on the leading edge but not at midspan because of the longitudinal temperature gradient. Lastly, detailed computer plots for the seven combinations are presented at the times of both maximum and minimum longitudinal strain

Comparison of NASTRAN and ISO3DQ Analysis

The comparison of the analyses of the single-edge wedge using the fine mesh model (fig. 1(b)) and NASTRAN with the coarse mesh model (fig. 1(c)) and ISO3DQ is given in figure 4. The comparison shows very good agreement. Both analyses were independently performed for NASA TAZ-8A alloy after 15 seconds of fluidized bed heating. This alloy and time increment were selected as being approximately the most severe combination of all those studied to accentuate any differences between analyses.

Figure 4(a) gives the normal x-, y-, and z-displacements along the leading and trailing edges. The greatest difference between the normal displacements as determined by the two methods is the x-displacement with the analyses for the other two displacements almost coinciding. However, comparing the net change between the leading and trailing edge x-displacements for the two analyses shows very similar results.

Figure 4(b) gives the longitudinal stress along the midchord at about one-quarter span which was the critical location for this combination. These very good comparative results show that both the leading and trailing edges are in compression. This is due to the manner of testing in that the specimens were stacked so that they were heated and cooled from both the leading and trailing edges. A force balance of this cross-section showed that equilibrium requirements were satisfied.

This comparison confirmed that the ISO3DQ program using a coarse mesh model was sufficiently accurate to obtain very good quantitative results. It also gave confidence in the use of this specialized blade and disk stress analysis program.

Critical Locations

Results for the seven analyzed combinations at the two critical locations (symmetrical about midspan) as a function of time after immersion into the fluidized beds are given in figure 5. This figure shows the temperature, and longitudinal strain and stress as a function of cycle time which occur at both critical locations on the leading edge.

In figure 5, the temperature is the nodal temperature at the critical locations on the leading edge as determined from the temperature loading that was input to the ISO3DQ program. The procedure used to determine this temperature is given in the section ISO3DQ Computer Program.

Both the longitudinal leading edge stress and strain show very steep gradients for about the first 10 seconds of immersion in both the heating or cooling beds. The results show that the leading edge goes into compression upon immersion into the heating bed. As the specimen reaches a steady-state condition, the stresses and strains approach zero. Upon immersion into the cooling bed, the leading edge goes into tension followed by a gradual drop-off to low stress and strain by the end of the cooling cycle.

The maximum longitudinal strainrange for the combinations analyzed varied from 0.35 to 0.56 percent. NASA TAZ-8A alloy demonstrated the highest strainrange of 0.56 percent. For 316 stainless steel the strainrange varied from 0.35 to 0.51 percent as the heating bed temperature increased. All three examined combinations of A-286 alloy exhibited strainranges of about 0.37 percent.

Due to symmetry, the analysis showed two critical locations on the leading edge which were either 2.5 or 3.33 cm (1.0 or 1.3 in.) away from midspan for each of the seven combinations evaluated. Preliminary experimental data in fluidized bed tests for some of the combinations indicate that cracks are initiated in this region.

The leading edge of the single-edge wedge is in a uniaxial state of stress. On the free surfaces, the normal x- and y-stresses (refer to fig. 1(c) for the axes convention) are zero. Therefore, the effective stress at the leading edge is equal in magnitude to the longitudinal z-stress. The x- and y-strains at the leading edge equal:

$$\epsilon_x = \epsilon_y = -\nu\epsilon_z \tag{1}$$

where ϵ = strain in x-, y-, or z-direction, and ν = Poisson's ratio. By definition (ref. 24) effective strain is

$$\epsilon_{eff} = \frac{\sqrt{2}}{3}\sqrt{(\epsilon_1 - \epsilon_2)^2 + (\epsilon_2 - \epsilon_3)^2 + (\epsilon_3 - \epsilon_1)^2} \tag{2}$$

where 1, 2, and 3 refer to the principal directions. Since the shear strains are zero at the leading edge, the normal strains equal the principal strains. Substituting eq. (1) in eq. (2) gives the effective strain at the leading edge as:

$$\epsilon_{eff} = \frac{2(1+\nu)}{3}\epsilon_z \tag{3}$$

Minimum and Maximum Longitudinal Strain

Results for the seven analyzed combinations at the time increment of minimum and maximum longitudinal strain are shown in figures 6 and 7 respectively. The complete distribution of temperature and also normal, shear, and effective stresses and strains are shown over the complete midchord plane of the wedge. The notation used is conventional elasticity notation with the axes convention as given in figure 1. The assumption of constant temperature through the thickness of the wedge results in zero y-stress over the midchord. For this reason the y-stress plot is not presented. The minimum (largest compressive) longitudinal strain always occurred during heating and the maximum longitudinal strain always occurred during the cooling part of the cycle. These plots were made utilizing

the PROUT3 program. These results show the reflective symmetry about midspan. These plots in addition to those in figure 5 will be used for further evaluation of various life prediction theories such as strainrange partitioning.

SUMMARY OF RESULTS AND CONCLUSIONS

The elastic stress analyses for a single-edge wedge geometry specimen cycled in fluidized beds were determined using three-dimensional finite-element techniques. The analyses were performed as a joint program of the NASA Lewis Research Center and the Air Force Aero Propulsion Laboratory (AFAPL). The NASA TAZ-8A alloy was analyzed using the NASTRAN computer program with a fine mesh for a severe heating time increment. The AFAPL used the ISO3DQ program with a coarse mesh model for this combination as well as all other combinations. A total of seven combinations consisting of three alloys and four cycling conditions were considered. The alloys were NASA TAZ-8A, 316 stainless steel, and A-286. The cycling condition for NASA TAZ-8A alloy was alternate 3 minute immersions in cold and hot beds maintained at 316° and 1088° C (600° and 1990° F) respectively. The three cycling conditions for both other alloys were alternate 4 minute immersions in a cooling bed always maintained at 21° C (70° F) and a heating bed maintained at one of three temperatures The temperatures were 740°, 850°, or 960° C (1364°, 1562°, or 1760° F). Specific major results are as follows:

1. The analyses showed the leading edge of the single-edge wedge goes into compression when immersed into the heating bed followed by tension when immersed into the cooling bed. Steep stress and strain gradients occurred during the first 10 seconds of immersion in either bed. For example, 0.35 percent strain was noted for NASA TAZ-8A alloy during the initial six seconds immersion in the heating bed.

2. The maximum longitudinal strainrange (algebraic difference between maximum and minimum longitudinal strain) for the seven combinations considered varied from 0.35 to 0.56 percent.

3. The two locations of the maximum longitudinal strainrange at the leading edge of each wedge were either 2.5 or 3.3 cm (1.0 or 1.3 in.) away from midspan for the seven combinations examined. Experimental test data for the combinations that have cracked indicate that the cracks initiated at these locations.

4. The comparison of the analyses using a fine mesh model (192 elements) and NASTRAN with a coarse mesh model (24 elements) and ISO3DQ showed very good agreement for the single condition checked.

5. The results from this investigation can be used for further evaluation of various life prediction theories such as strainrange partitioning.

REFERENCES

1. Bizon, Peter T.; and Spera, David A.: Comparative Thermal Fatigue Resistances of Twenty-Six Nickel- and Cobalt-Base Alloys. NASA TN D-8071, 1975.
2. Bizon, Peter T., and Oldrieve, Robert E.: Thermal Fatigue Resistance of NASA WAZ-20 Alloy With Three Commercial Coatings. NASA TM X-3168, 1975.
3. Spera, David A., Howes, Maurice A. H.; and Bizon, Peter T.: Thermal Fatigue Resistance of 15 High-Temperature Alloys Determined by the Fluidized-Bed Technique. NASA TM X-52975, 1971.
4. Howes, Maurice A. H.: Thermal Fatigue Data on 15 Nickel- and Cobalt-Base Alloys. (IITRI-B6078-38, IIT Research Institute; NASA Contract NAS3-9411.) NASA CR-72738, 1970.
5. Howes, Maurice A. H.: Additional Thermal Fatigue Data on Nickel- and Cobalt-Base Superalloys, Part 1. (IITRI-B6107-34-Pt-1, IIT Research Institute; NASA Contract NAS3-14311.) NASA CR-121211, 1973.
6. Howes, M. A. H.: Additional Thermal Fatigue Data on Nickel- and Cobalt-Base Superalloys, Part 2. (IITRI-B6107-34-Pt-2, IIT Research Institute; NASA Contract NAS3-14311.) NASA CR-121212, 1973.
7. Howes, M. A. H.: Thermal Fatigue and Oxidation Data on TAZ-8A, MAR-M 200, and Udimet 700 Superalloys. (IITRI-B6124-21, IIT Research Institute; NASA Contract NAS3-17787.) NASA CR-134775, 1975.

8. Hill, V. L., and Humphreys, V. E. Thermal Fatigue and Oxidation Data of Superalloys Including Directionally Solidified Eutectics. (IITRI-B6124-48, IIT Research Institute, NASA Contract NAS3-17787.) NASA CR-135272, 1977.

9. Hill, V. L.; and Humphreys, V. E. Thermal Fatigue and Oxidation Data for Alloy/Braze Combinations. (IITRI-B6134-25, IIT Research Institute, NASA Contract NAS3-18942.) NASA CR-135299, 1977.

10 Hirschberg, M. H.; and Halford, G. R. Use of Strainrange Partitioning to Predict High-Temperature Low-Cycle Fatigue Life. NASA TN D-8072, 1976.

11. Saltsman, J. F., and Halford, G. R. Application of Strainrange Partitioning to the Prediction of Creep-Fatigue Lives of AISI Types 304 and 316 Stainless Steel. J. Pressure Vessel Technol., vol. 99, no. 2, May 1977, pp. 264-271. (NASA TM X-71898, 1976.)

12. Hirschberg, M. H.; and Halford, G. R.. Strainrange Partitioning: A Tool for Characterizing High Temperature Low Cycle Fatigue - Materials Fatigue Test. NASA TM X-71691, 1975.

13. Halford, G. R.; Saltsman, J. F.; and Hirschberg, M. H. Ductility Normalized-Strainrange Partitioning Life Relations for Creep-Fatigue Life Prediction. NASA TM-73737, 1977.

14. Halford, G. R.; Hirschberg, M. H.; and Manson, S. S.: Creep Fatigue Analysis by Strain-Range Partitioning. NASA TM X-67838, 1971.

15. Spera, David A.; and Grisaffe, Salvatore, J.: Life Prediction of Turbine Components: On-Going Studies at the NASA Lewis Research Center. NASA TM X-2664, 1973

16. Fritz, Louis J., and Koster, W. P.: Tensile and Creep Rupture Properties of (16) Uncoated and (2) Coated Engineering Alloys at Elevated Temperatures. (Rept.-931-21300, Metcut Research Associates, Inc.; NASA Contract NAS3-18911.) NASA CR-135138, 1977.

17. Wolf, J., ed.: Aerospace Structural Metals Handbook. Mechanical Properties Data Center; Belfour Stulen, Inc., 1978. AFML-TR-68-115, Revised.

18. The NASTRAN Theoretical Manual (Level 16.0). NASA SP-221(03), 1976.

19. The NASTRAN Programmer's Manual (Level 16.0). NASA SP-223(03), 1976.

20. The NASTRAN User's Manual (Level 16.0 Supplement). NASA SP-222(03), 1976.

21. The NASTRAN Demonstration Problem Manual (Level 16.0). NASA SP-224(03), 1976.

22. Alderson, R. G., et. al.: Turbine Engine Components Stress Simulation Program. AiResearch-74-210816(32), AiResearch Manufacturing Co., 1977. (AFAPL-TR-77-72, AD-B027424L.)

23. User's Manual - Programs MESH3, ISO3DQ, and PROUT3 Turbine Engine Components Stress Simulation Program. Rept. 74-210860(2)-1A, AiResearch Mfg. Co., Mar. 1977. (Air Force Aero Propulsion Laboratory Contract F33615-74-C-2012.)

24. Hoffman, Oscar; and Sachs, George: Introduction to the Theory of Plasticity for Engineers. McGraw-Hill Book Co., Inc., 1953, p. 28.

TABLE I. - ALLOYS AND CONDITIONS ANALYZED

Alloy	Fluidized bed temperatures				Immersion time in each bed, sec
	Heating		Cooling		
	°C	°F	°C	°F	
NASA TAZ-8A	1088	1990	316	600	180
316 stainless steel	740	1364	21	70	240
	850	1562	↓	↓	↓
	960	1760			
A-286	740	1364			
	850	1562			
	960	1760	↓	↓	↓

TABLE II - TEMPERATURE INDEPENDENT

ALLOY PROPERTIES

Alloy	Poisson's ratio	Density	
		gm/cm^3	$lb/in.^3$
NASA TAZ-8A	0.3166	8.636	0.312
316 stainless steel	.2885	8.027	.290
A-286	.2628	7.916	.286

TABLE III - TEMPERATURE DEPENDENT ALLOY PROPERTIES

		NASA TAZ-8A				316 stainless steel				A-286			
		E^a		α^b		E^a		α^b		E^a		α^b	
^oC	^oF	N/m^2	psi	$\frac{m/m}{^oC}$	$\frac{in./in}{^oF}$	N/m^2	psi	$\frac{m/m}{^oC}$	$\frac{in/in}{^oF}$	N/m^2	psi	$\frac{m/m}{^oC}$	$\frac{in/in}{^oF}$
-17 8	0	208×10^9	30.1×10^6	10.3×10^{-6}	$5\ 7\times10^{-6}$	199×10^9	28.8×10^6	$15\ 3\times10^{-6}$	$8\ 5\times10^{-6}$	201×10^9	$29\ 2\times10^6$	$16\ 2\times10^{-6}$	$9\ 0\times10^{-6}$
37.8	100	206	29.9	10.6	5.9	197	28 5	15 5	8 6	199	28 8	16 4	9 1
93 0	200	205	29.8	11.0	6 1	194	28 1	15 7	8 7	195	28 3	16 6	9 2
149	300	205	29.7	11.5	6.4	190	27 6	15 9	8 85	190	27 5	16 7	9 3
204	400	203	29.5	11.9	6 6	186	27.0	16 2	9 0	186	27 0	16 9	9 4
260	500	202	29.3	12.1	6.7	181	26.2	16 6	9 2	183	26 5	17 0	9 45
316	600	201	29.1	12.1	6 7	177	25.6	16 9	9.4	178	25 8	17 2	9 55
371	700	199	28.9	12.2	6.8	172	24 9	17 3	9 6	174	25 2	17 4	9 65
427	800	198	28.7	12 4	6 9	166	24 1	17 6	9.8	170	24 6	17 6	9 75
482	900	197	28.5	12.6	7.0	162	23 5	18 0	10 0	164	23 8	17 6	9 8
538	1000	194	28.2	12.8	7 1	157	22.7	18 4	10 2	160	23 2	17 8	9 9
593	1100	192	27.9	12.8	7.1	152	22 0	18.5	10 25	155	22 5	18 2	10 1
649	1200	190	27.5	13 0	7.2	145	21.0	18.5	10.3	152	22 0	18 4	10 2
704	1300	187	27 1	13.1	7 3	139	20.2	18.7	10 4	147	21 3	18.5	10 25
760	1400	183	26.5	13.3	7 4	137	19 8	18 9	10 5	141	20 5	18 5	10 3
816	1500	178	25.8	13.5	7 5	132	19.2	19 0	10 55	134	19.5	18.7	10 4
871	1600	168	24.3	13.9	7 7	130	18.9	19.1	10.6	130	18 8	18 9	10 5
927	1700	146	21 2	14.2	7 9	128	18.6	19 2	10 65	124	18 0	19 1	10 6
982	1800	139	20.2	14.6	8.1	126	18 3	19 3	10 7	117	17 0	19 3	10 7
1038	1900	133	19.3	14.9	8.3	124	18.0	19 4	10 75	110	15 9	19 4	10 8
1093	2000	128	18.5	15.3	8.5	123	17 8	19.4	10.8	102	14 8	19.6	10 9

[a] E modulus of elasticity.

[b] α mean coefficient of thermal expansion from room temperature to indicated temperature.

TABLE IV. - TEMPERATURE VARIATION ALONG SPAN

[$T_{x, z} = T_{x, ms} (Az^2 + Bz + C)$, where $T_{x, z}$ is the temperature at any x, z coordinate (see fig. 1), $T_{x, ms}$ is the temperature at the x coordinate at midspan, and z is the span coordinate, all temperatures in ^{o}F ($F = 9/5\ C + 32$).]

Time increment, sec	Heating bed			Cooling bed		
	A	B	C	A	B	C
0	-0.00870	0.0517	0.9205	-0.00666	0.03957	0.9427
3	.04401	-.2614	1.3891	-.01775	.1055	.8447
6	.03739	-.2221	1.3290	-.02384	.1416	.7911
9	.03688	-.2191	1.3372	-.02548	.1514	.7786
12	.03806	-.2261	1.3344	-.02731	.1622	.7622
15	.03695	-.2195	1.3300	-.02889	.1716	.7480
30	.02758	-.1638	1.2504	-.03047	.1810	.7338
45	.01769	-.1051	1.1630	-.03141	.1866	.7224
60	.01432	-.08506	1.1324	-.03442	.2044	.6905
75	.01006	-.05978	1.0934	-.03265	.1939	.7093
90	.00833	-.04948	1.0791	-.02867	.1703	.7440
105	.00557	-.03311	1.0528	-.02445	.1452	.7843
120	.00627	-.03722	1.0571	-.02276	.1352	.7981
135	.00440	-.02614	1.0415	-.01876	.1142	.8323
150	.00371	-.02205	1.0357	-.01533	.09107	.8622
165	.00297	-.01762	1.0285	-.01278	.07593	.8832
180	.00262	-.01553	1.0243	-.01212	.07198	.8876
195	↓	↓	↓	↓	↓	↓
210						
225						
240						

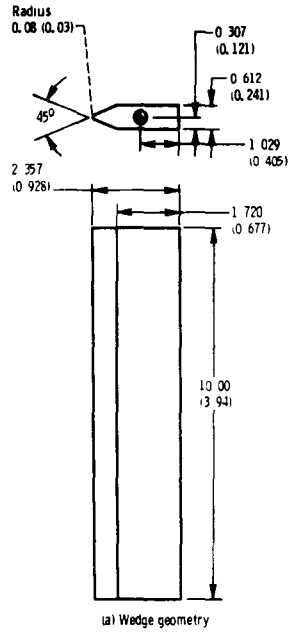

(a) Wedge geometry

Figure 1 - Single-edge wedge (All dimensions in cm (in) unless indicated otherwise)

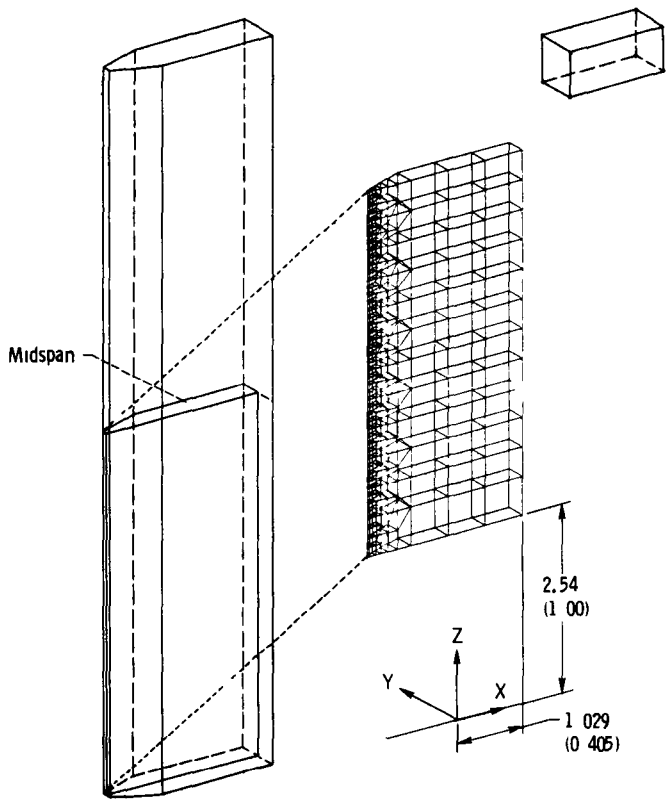

(b) Model and typical element used for NASTRAN analysis with coordinate convention

Figure 1 - Continued.

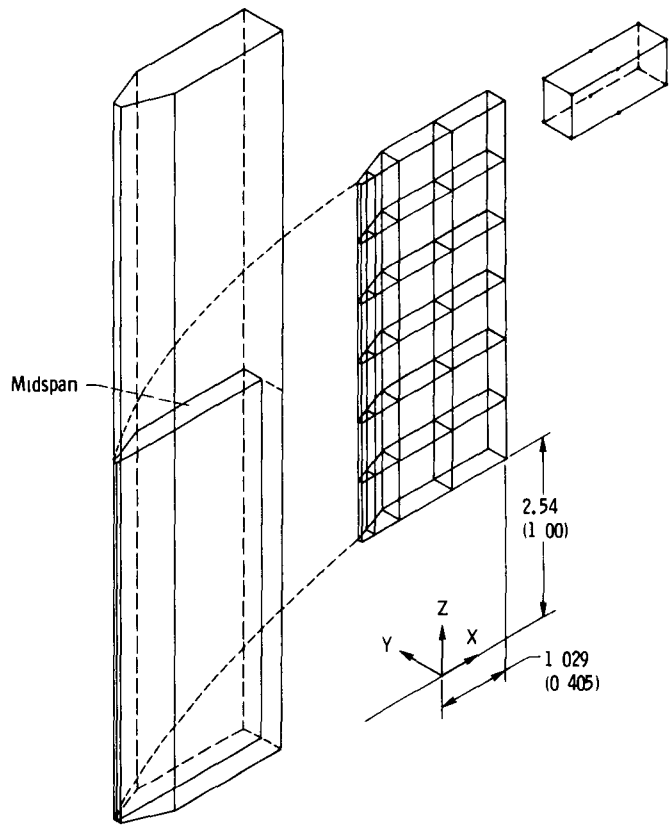

(c) Model and typical element used for IS03DQ analysis with coordinate convention

Figure 1 - Concluded

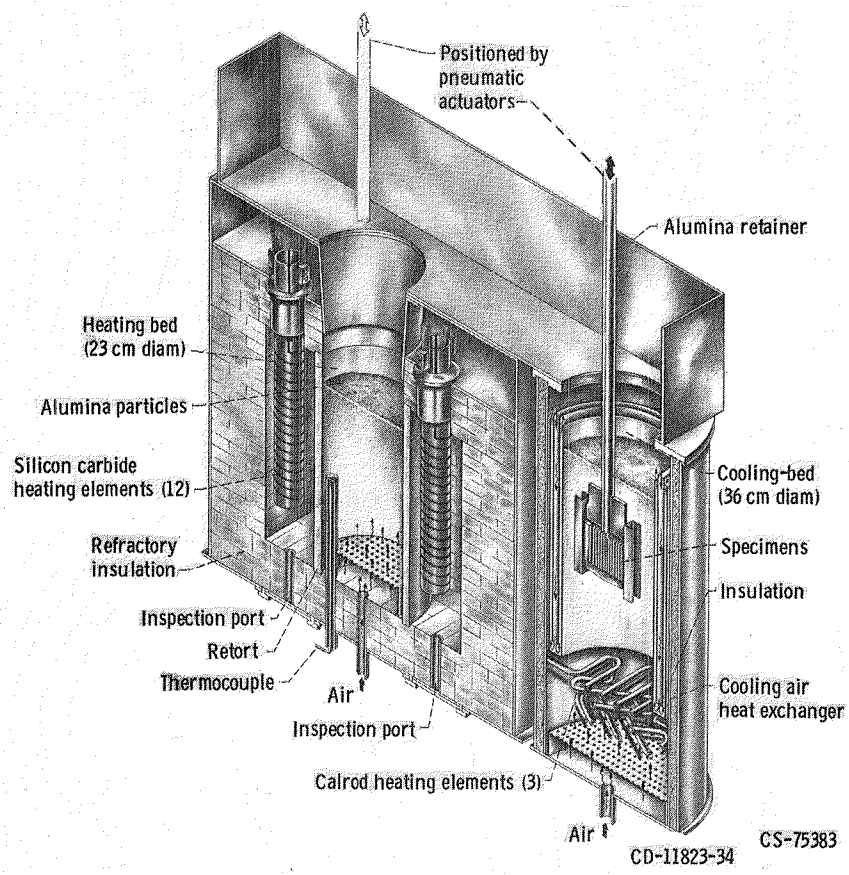

Figure 2. - Schematic of fluidized bed test facility.

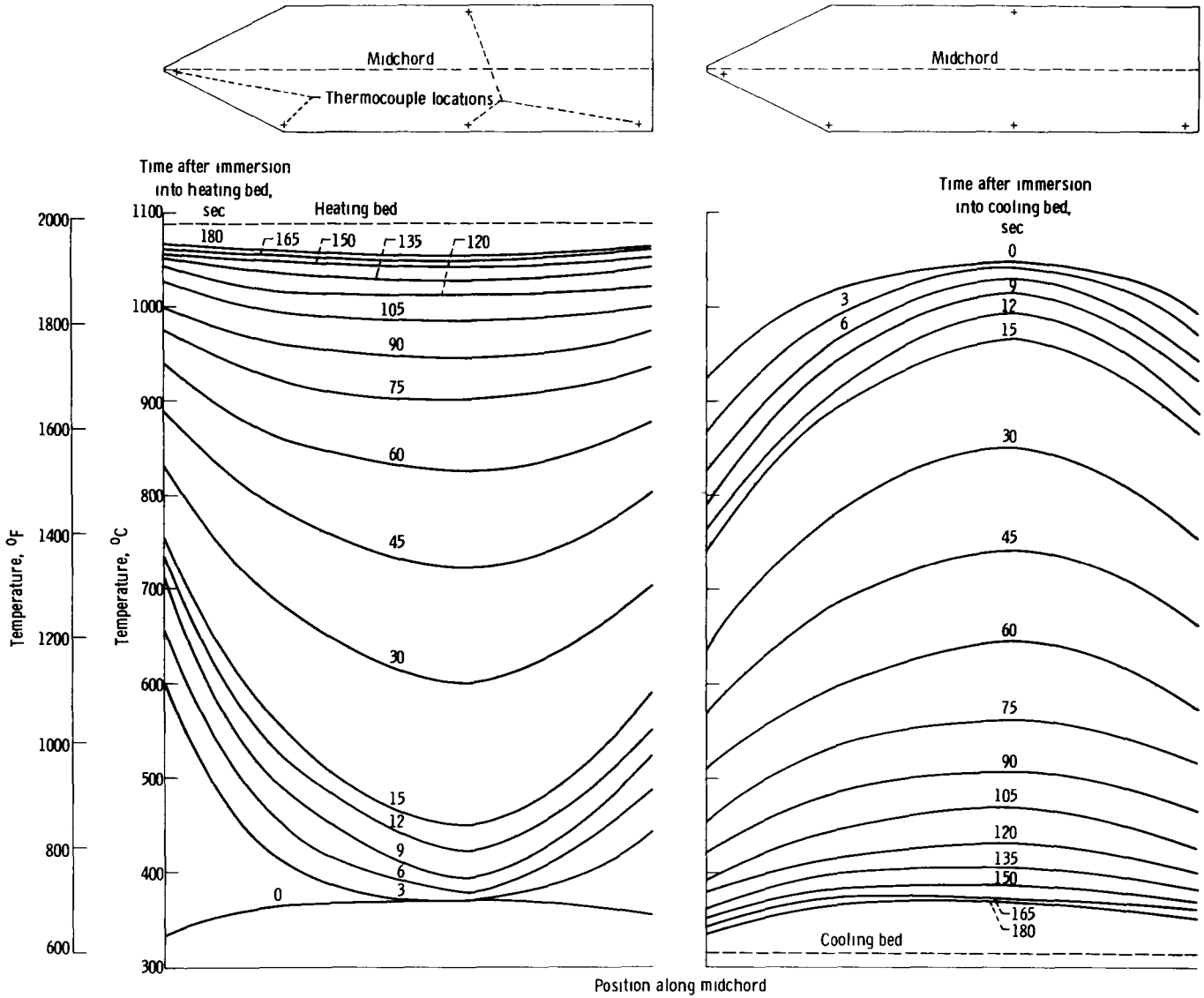

(a) NASA TAZ-8A alloy with the fluidized beds maintained at 1088° and 316° C (1990° and 600° F)

Figure 3 - Temperature of midchord at midspan at various times after immersion into the fluidized beds

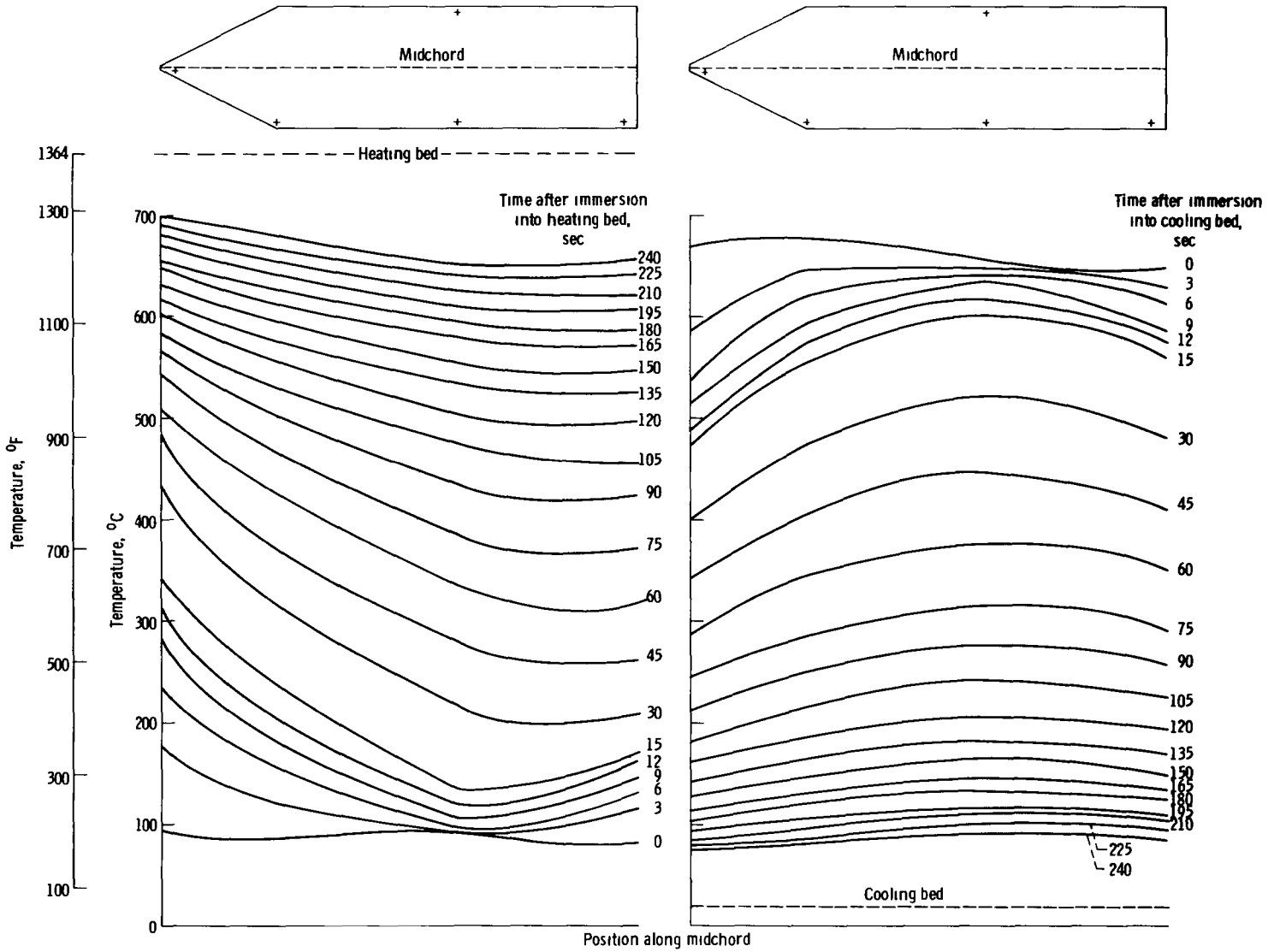

(b) 316 stainless steel alloy with the fluidized beds maintained at 740° and 21° C (1364° and 70° F)

Figure 3 - Continued

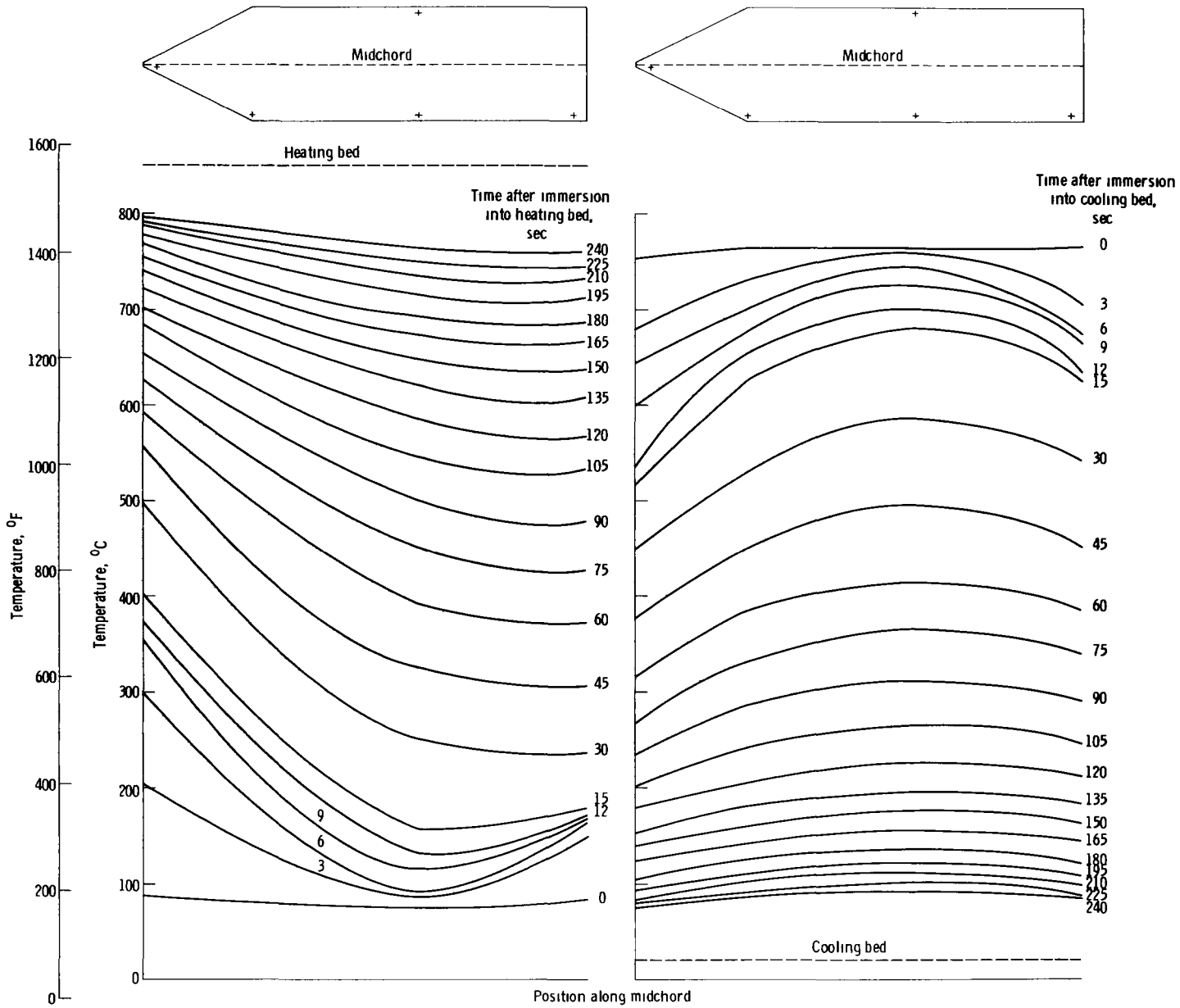

(c) 316 stainless steel alloy with the fluidized beds maintained at 850° and 21° C (1562° and 70° F)

Figure 3 - Continued

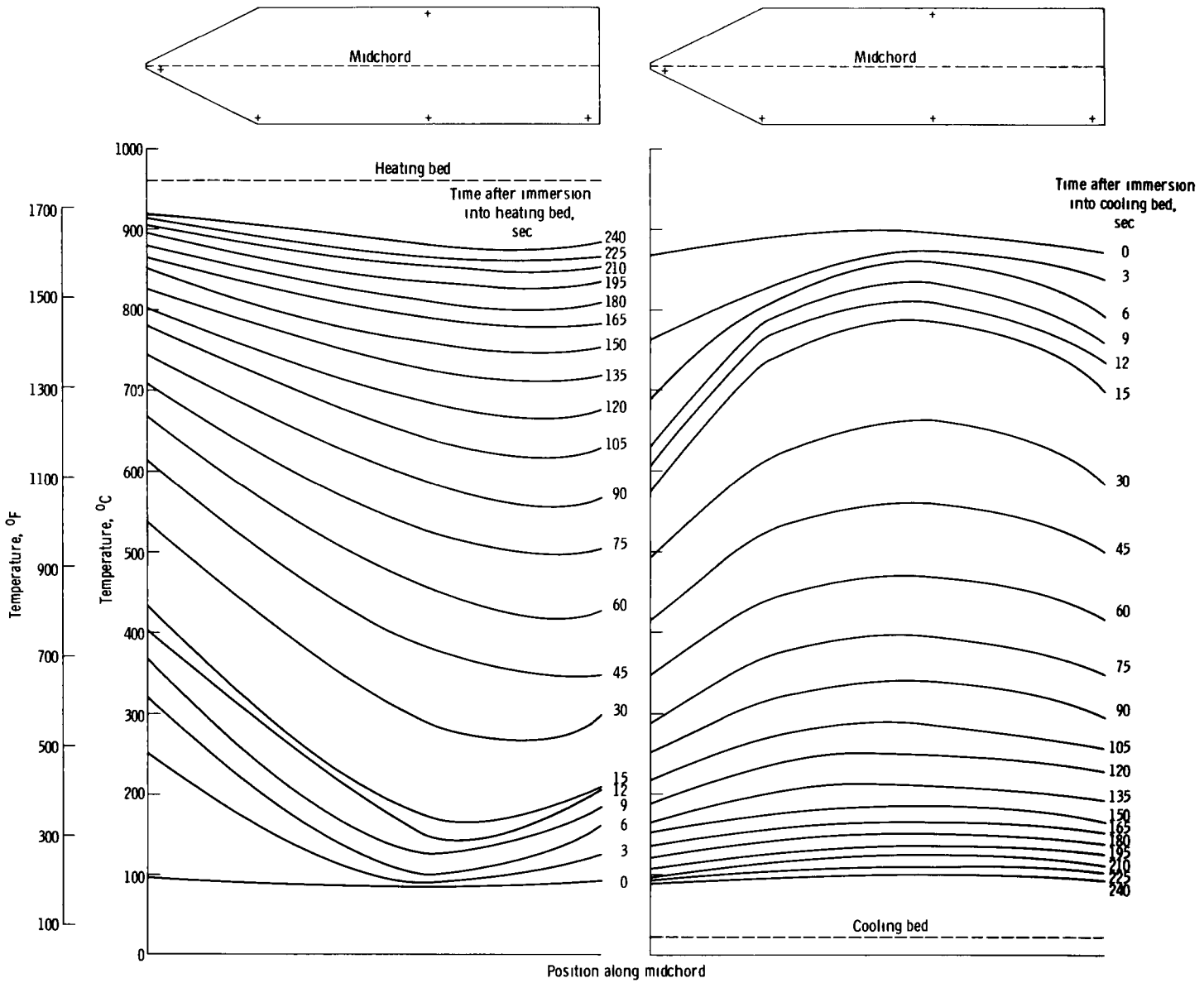

(d) 316 stainless steel alloy with the fluidized beds maintained at 960° and 21° C (1760° and 70° F)

Figure 3 - Continued

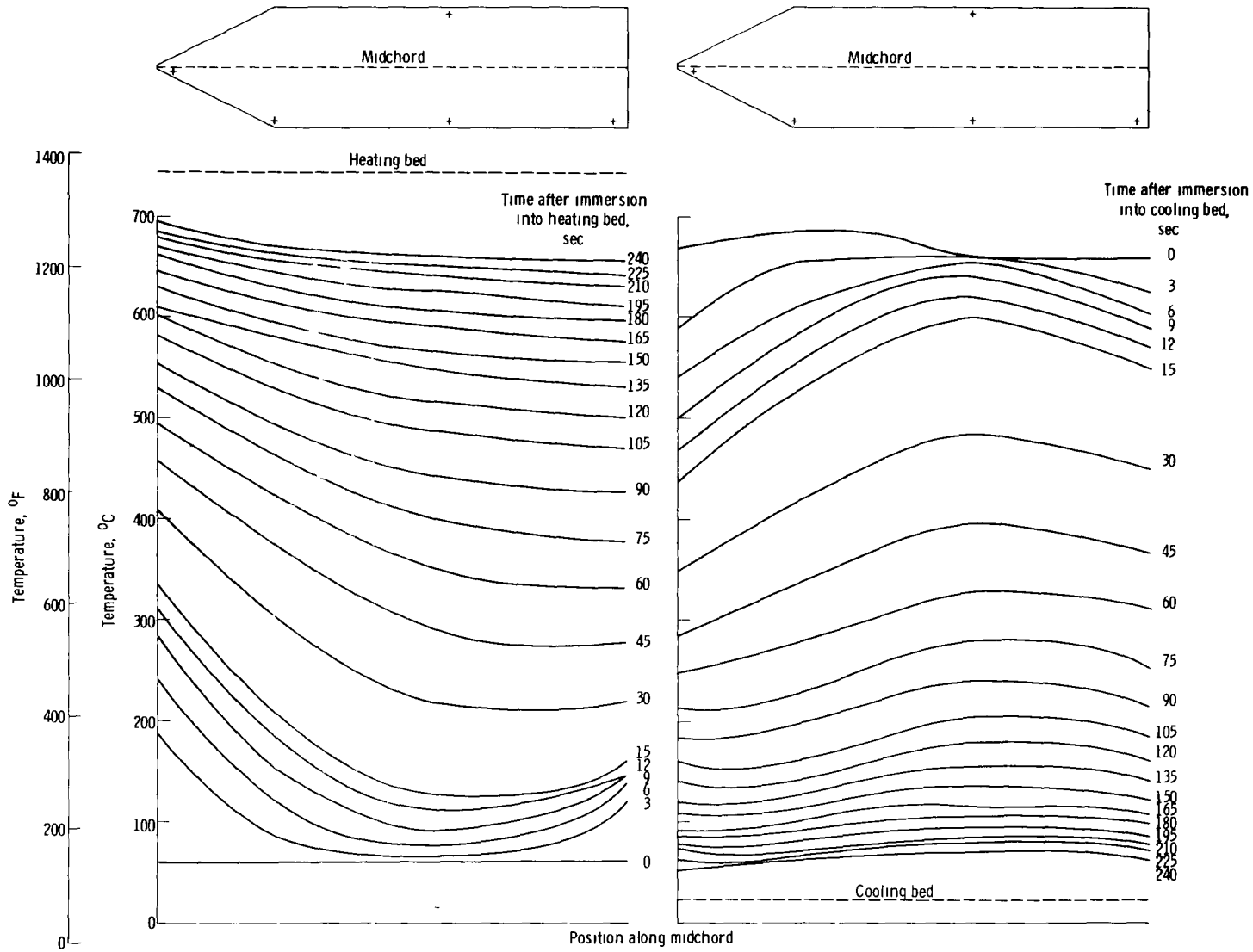

(e) A-286 alloy with the fluidized beds maintained at 740° and 21° C (1364° and 70° F)

Figure 3 - Continued

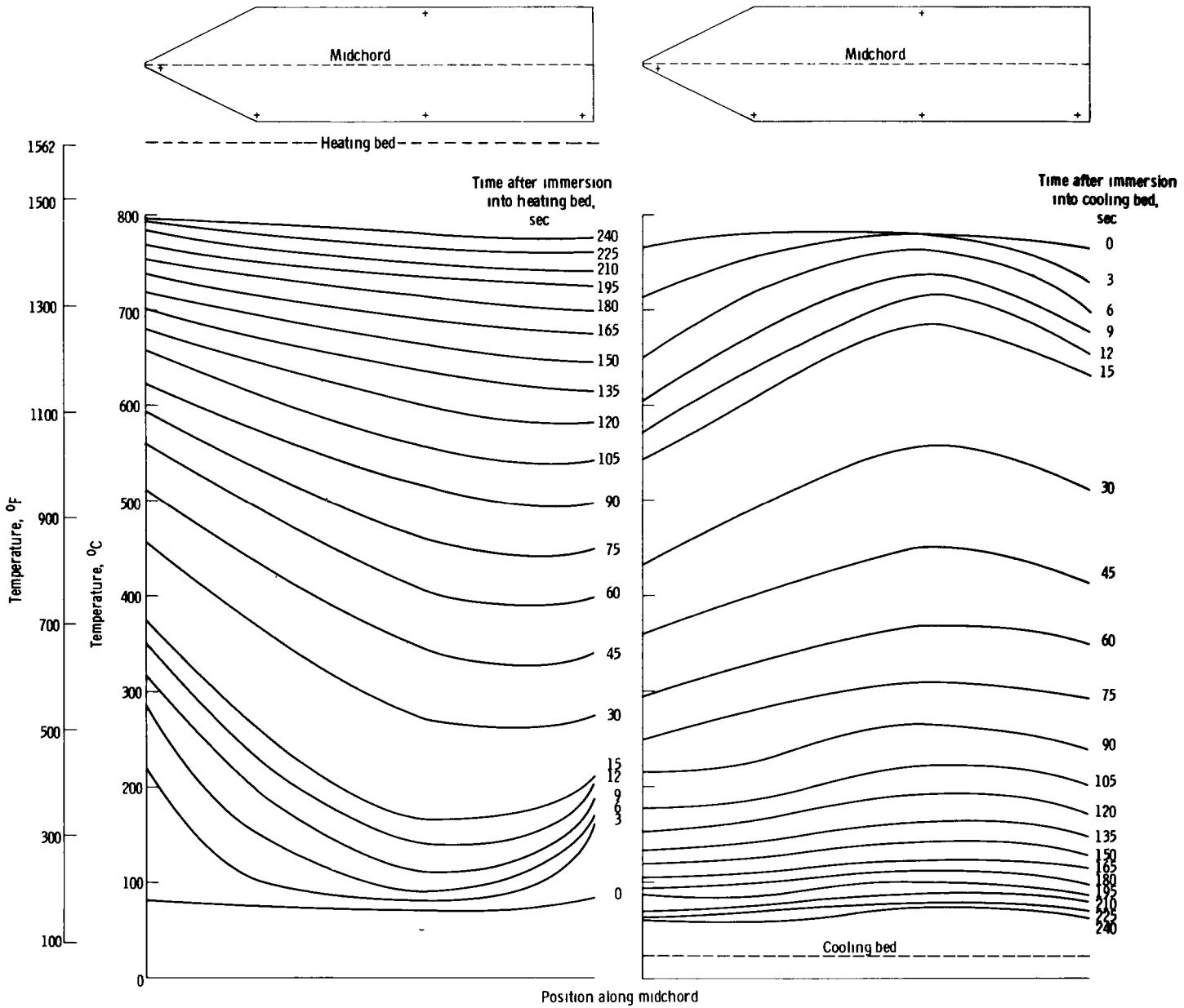

(f) A-286 alloy with the fluidized beds maintained at 850° and 21° C (1562° and 70° F)

Figure 3 - Continued

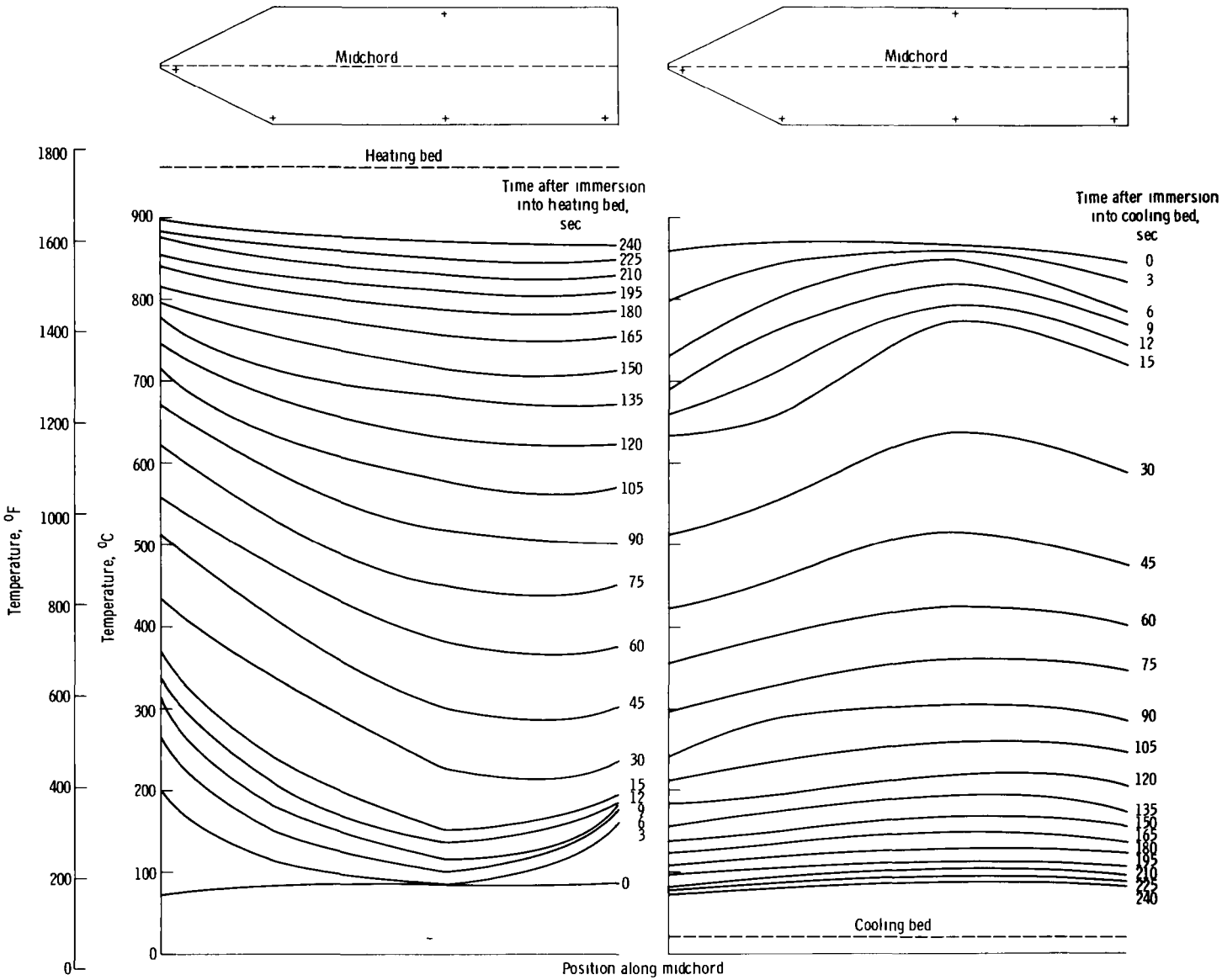

(g) A-286 alloy with the fluidized beds maintained at 960° and 21° C (1760° and 70° F)

Figure 3 - Concluded

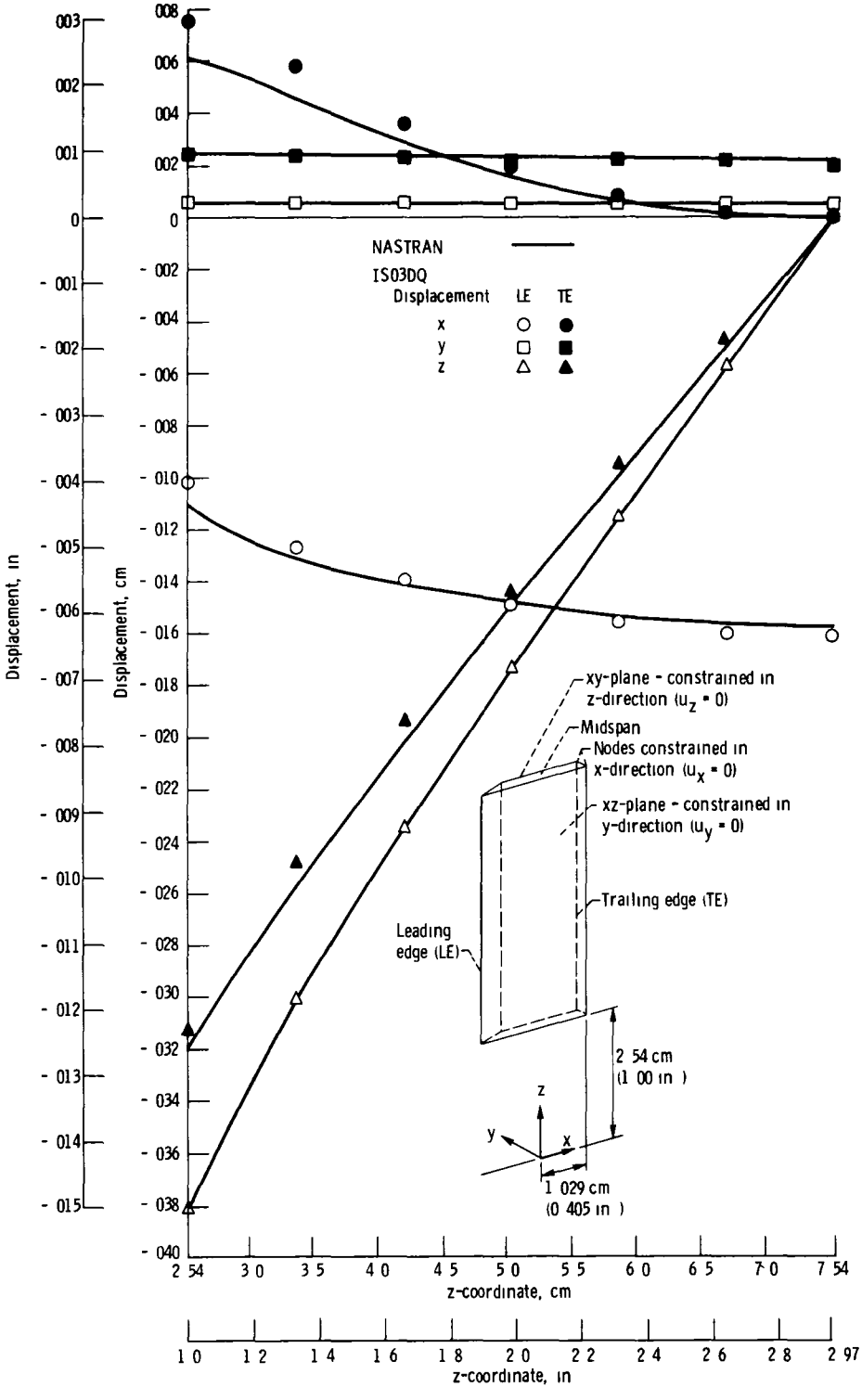

(a) Normal displacements

Figure 4 - Comparisons determined by using NASTRAN and IS03DQ computer programs (using the models in fig 1) for NASA TAZ-8A alloy after 15 seconds heating in the 1088° C (1990° F) fluidized bed

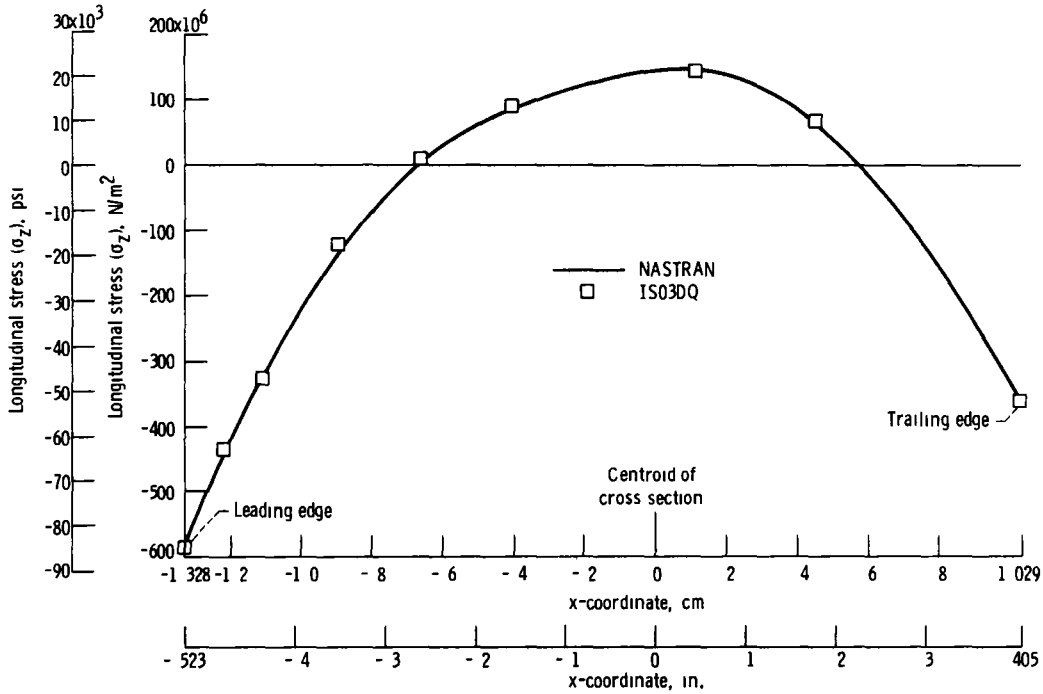

(b) Longitudinal stress (σ_z) along midchord at z = 5 1 cm (z = 2 01 in)

Figure 4 - Concluded

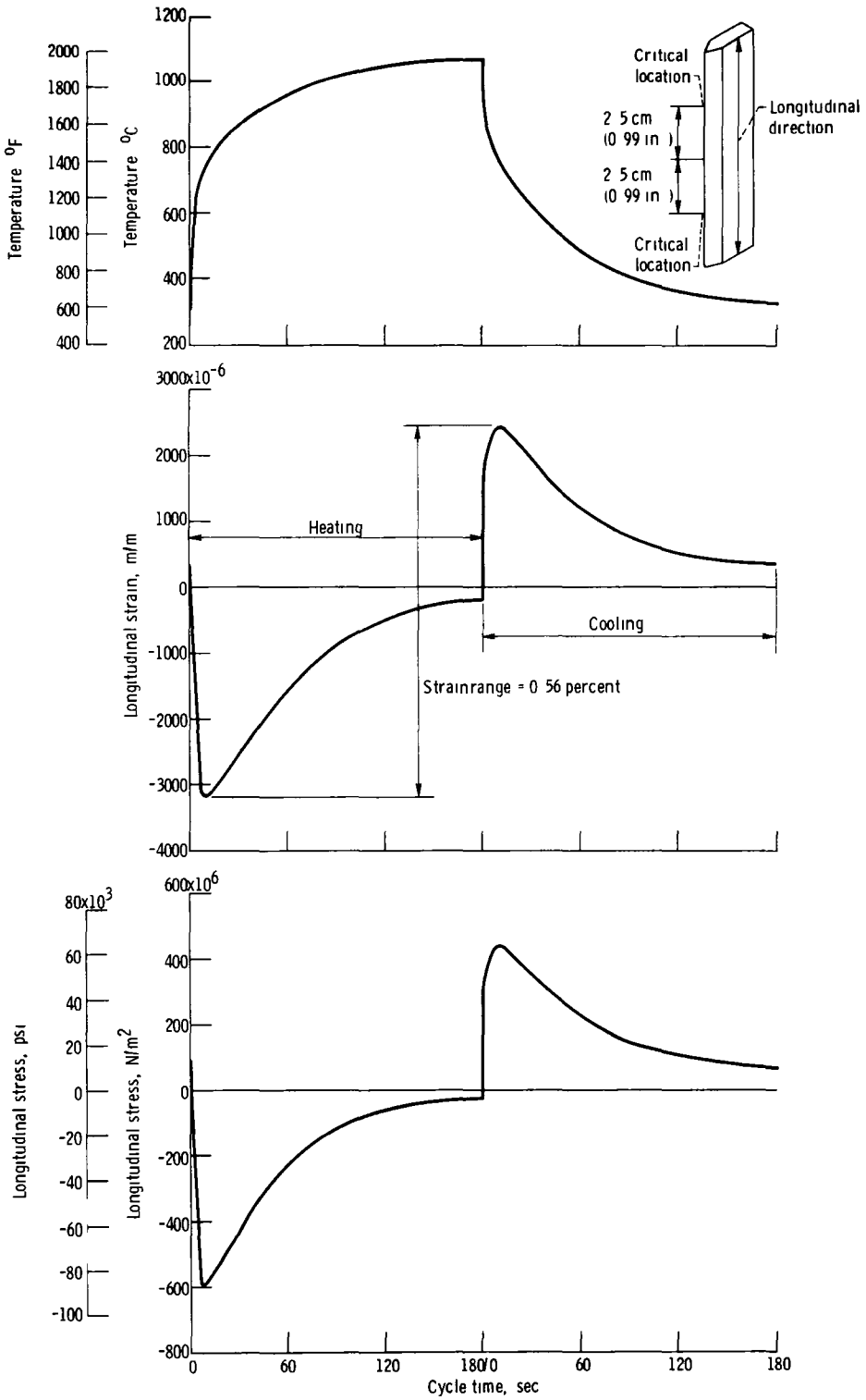

(a) NASA TAZ-8A alloy with the fluidized beds maintained at 1088° and 316° C (1990° and 600° F)

Figure 5 - Temperature, longitudinal strain, and longitudinal stress at critical locations during a typical fluidized bed cycle

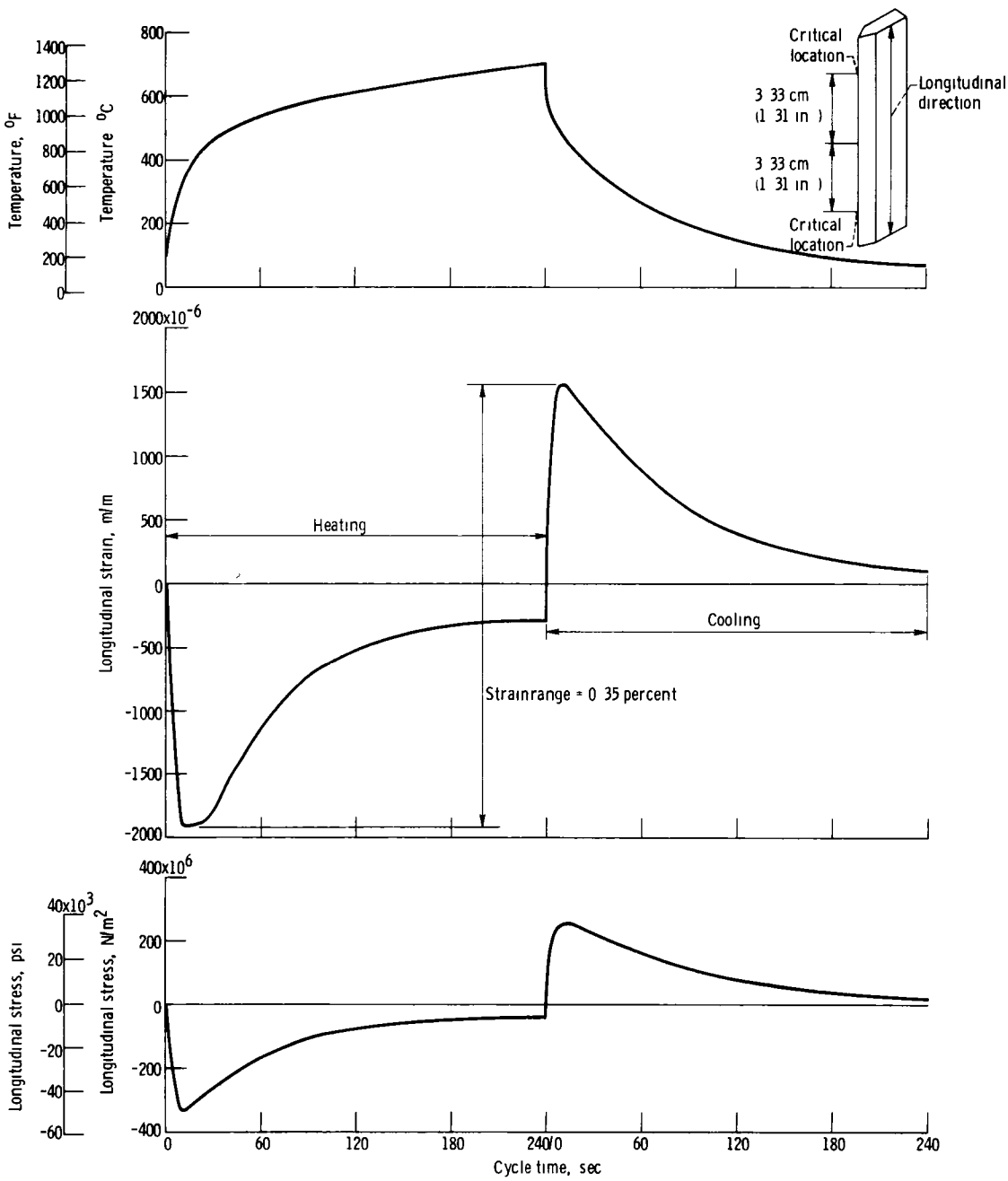

(b) 316 stainless steel alloy with the fluidized beds maintained at 740° and 21° C (1364° and 70° F)

Figure 5 - Continued

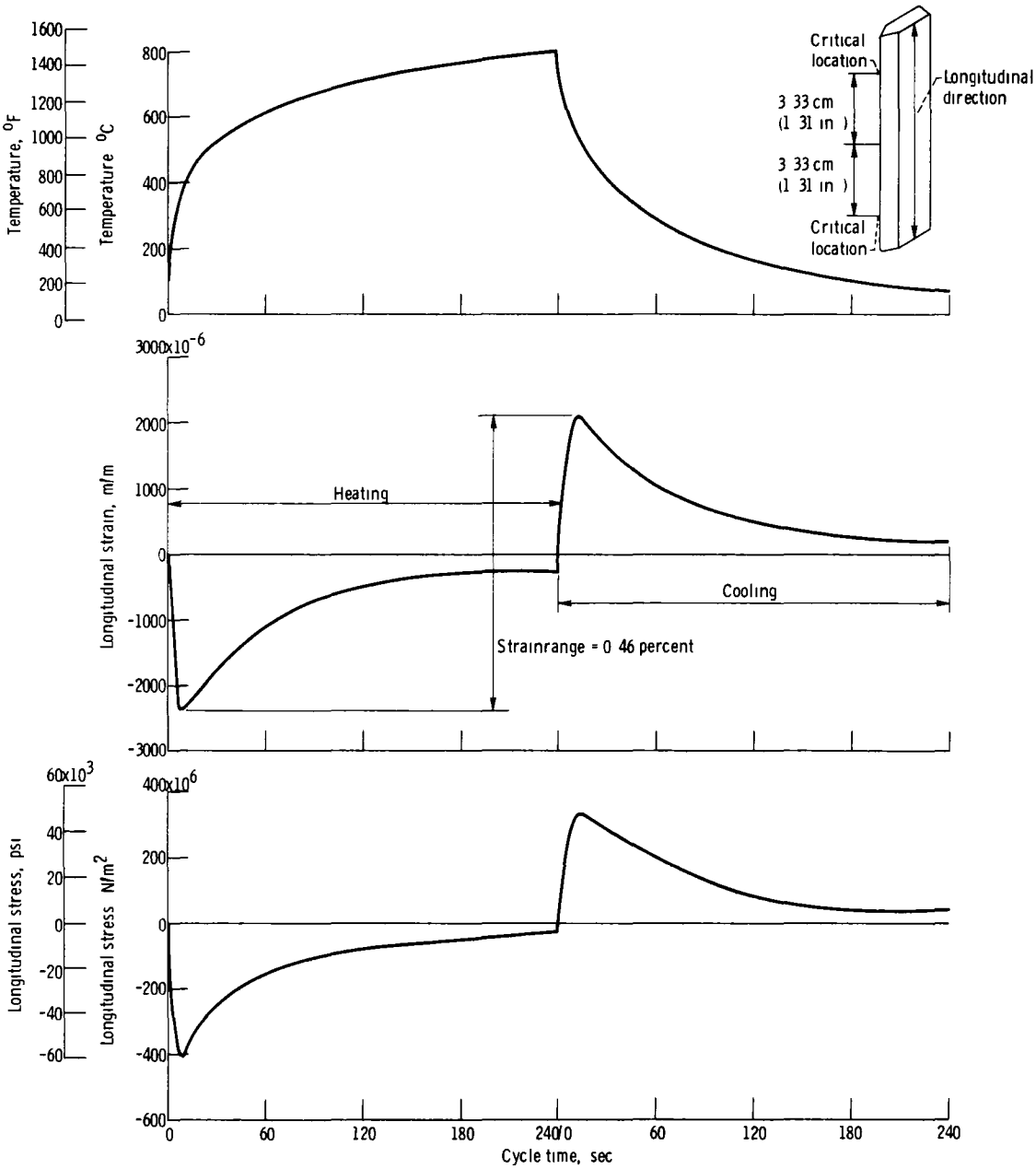

(c) 316 stainless steel alloy with the fluidized beds maintained at 850° and 21° C (1562° and 70° F)

Figure 5 - Continued

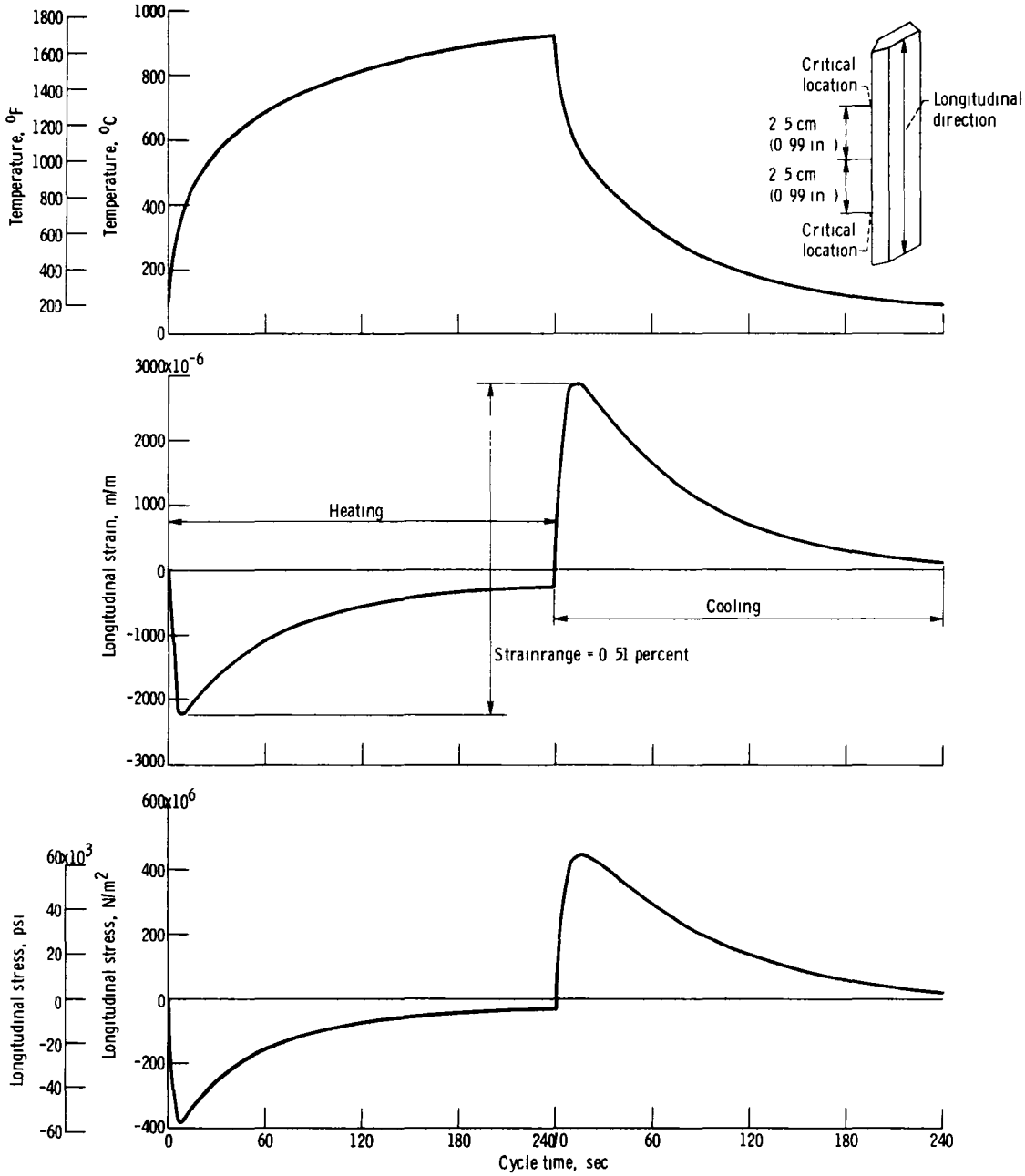

(d) 316 stainless steel alloy with the fluidized beds maintained at 960° and 21° C (1760° and 70° F)

Figure 5 - Continued

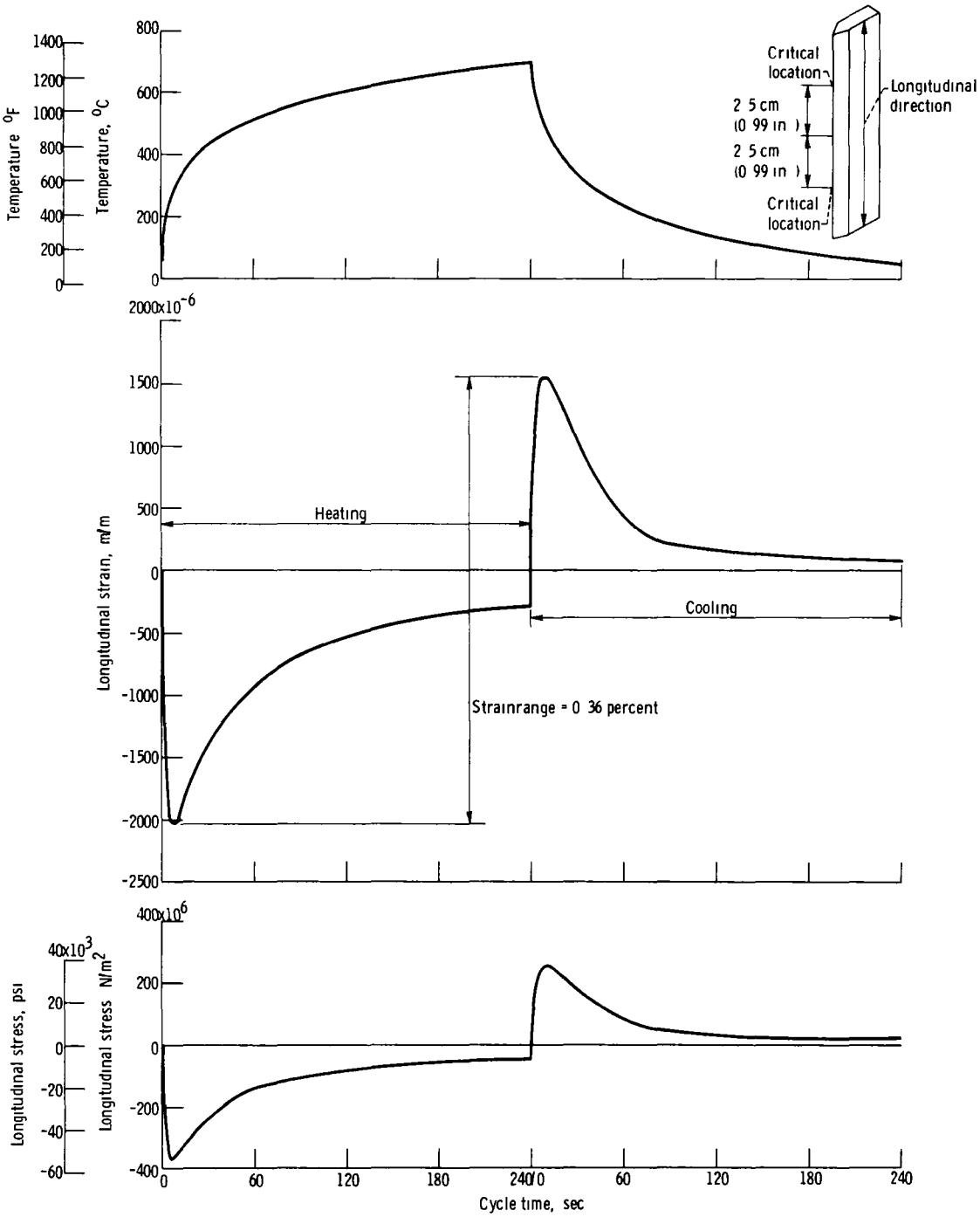

(e) A-286 alloy with the fluidized beds maintained at 740° and 21° C (1364° and 70° F)

Figure 5 - Continued

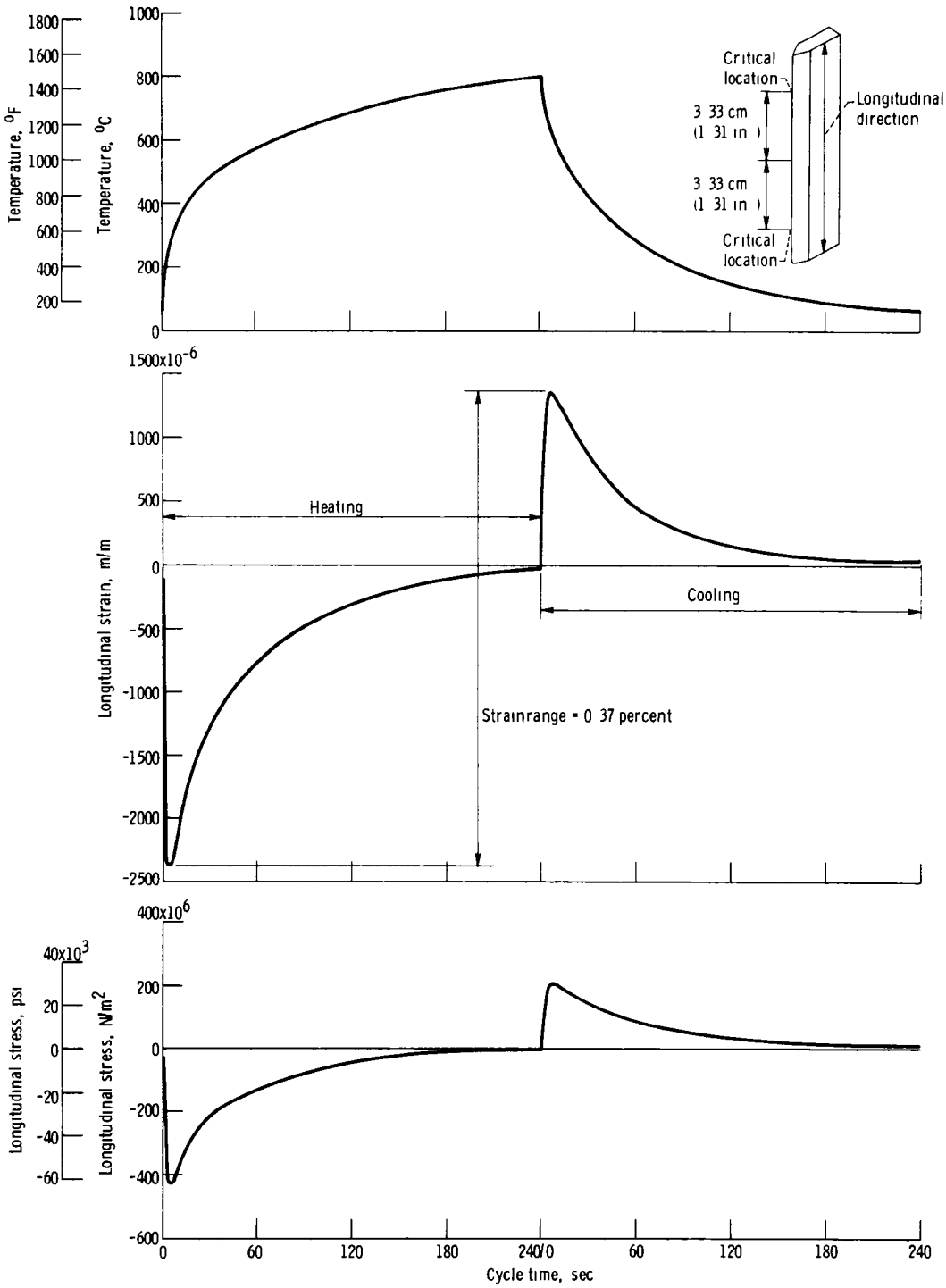

(f) A-286 alloy with the fluidized beds maintained at 850° and 21° C (1562° and 70° F)

Figure 5 - Continued

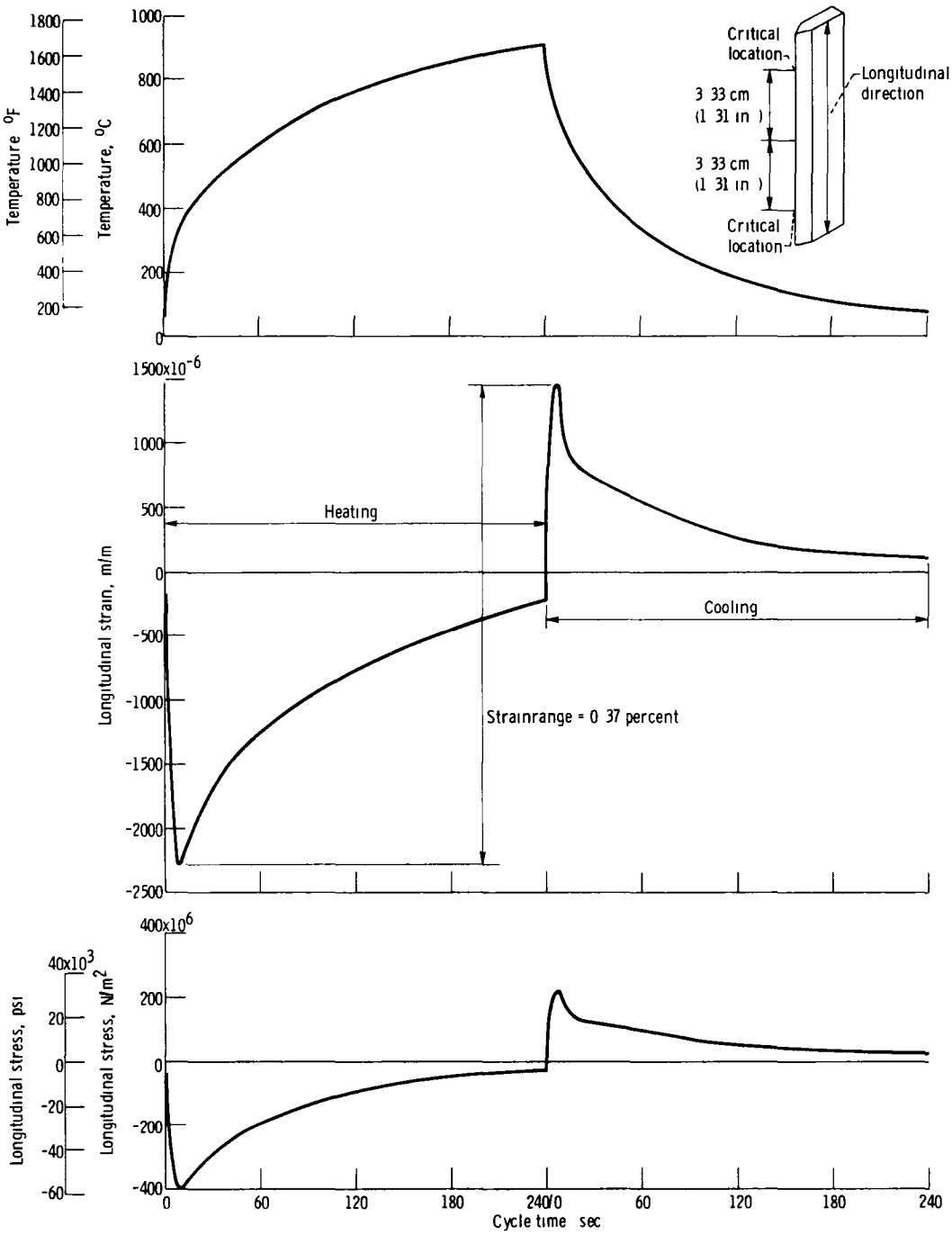

(g) A-286 alloy with the fluidized beds maintained at 960° and 21° C (1760° and 70° F)

Figure 5 - Concluded

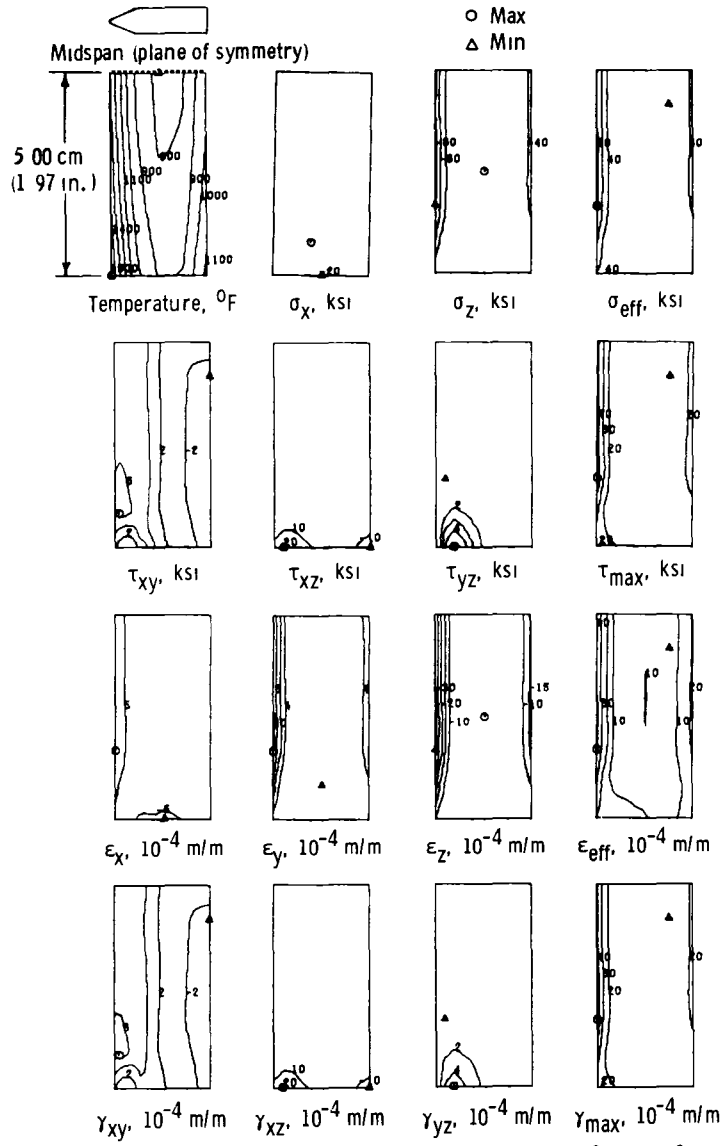

(a) NASA TAZ-8A alloy with fluidized beds maintained at 1088° and 316° C (1990° and 600° F) after 9 seconds immersion in the heating bed

Figure 6 - Temperature, stress, and strain distribution of midchord at time of minimum leading edge longitudinal strain (F = 9/5 C + 32)(1 ksi = 6 895x10^6 N/m^2)

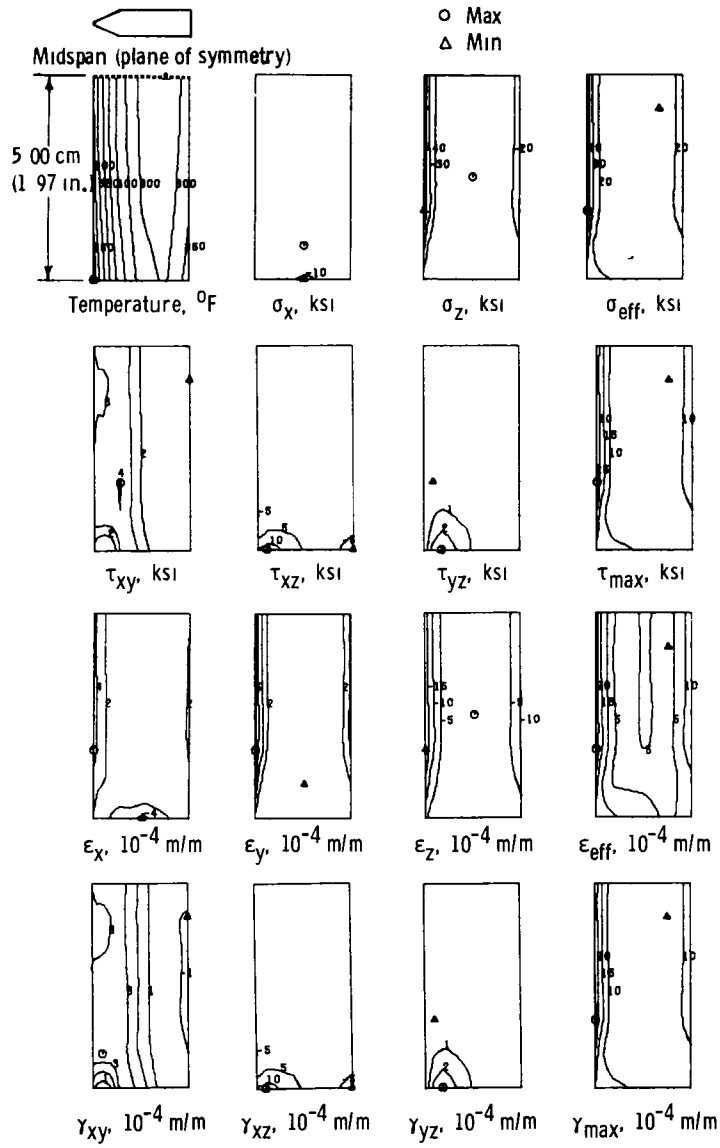

(b) 316 stainless steel alloy with the fluidized beds maintained at 740° and 21° C (1364° and 70° F) after 12 seconds immersion in the heating bed

Figure 6 - Continued.

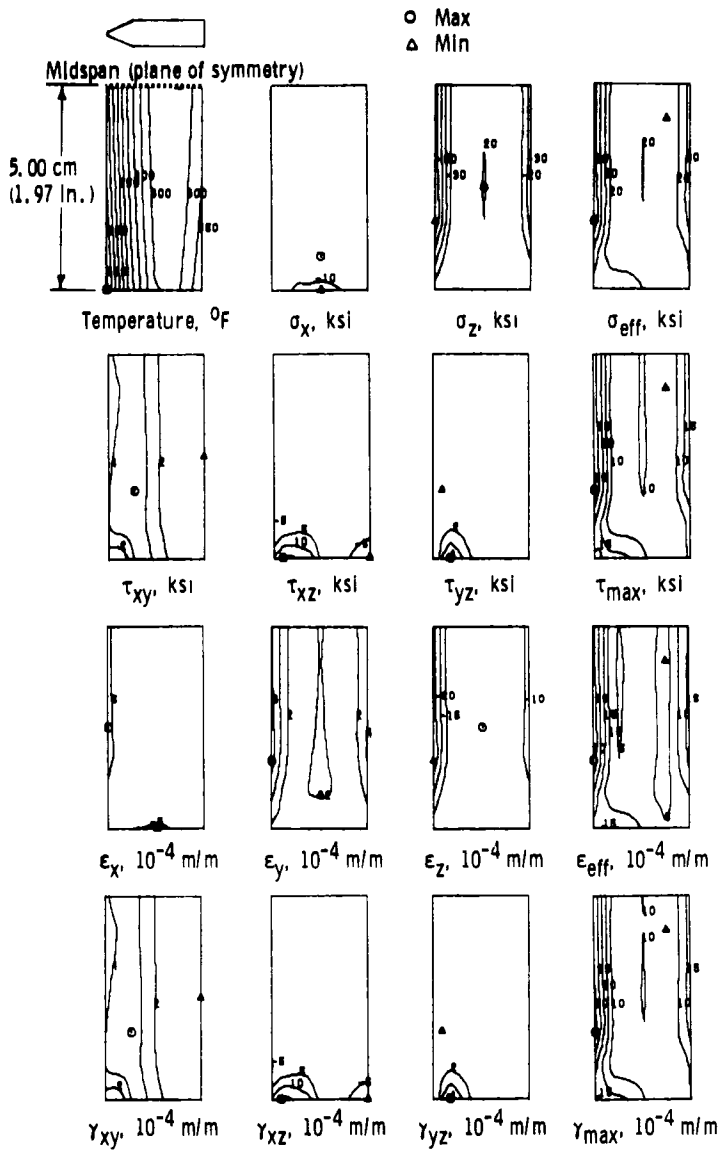

(c) 316 stainless steel alloy with the fluidized beds maintained at 850° and 21° C (1562° and 70° F) after 9 seconds immersion in the heating bed

Figure 6. - Continued

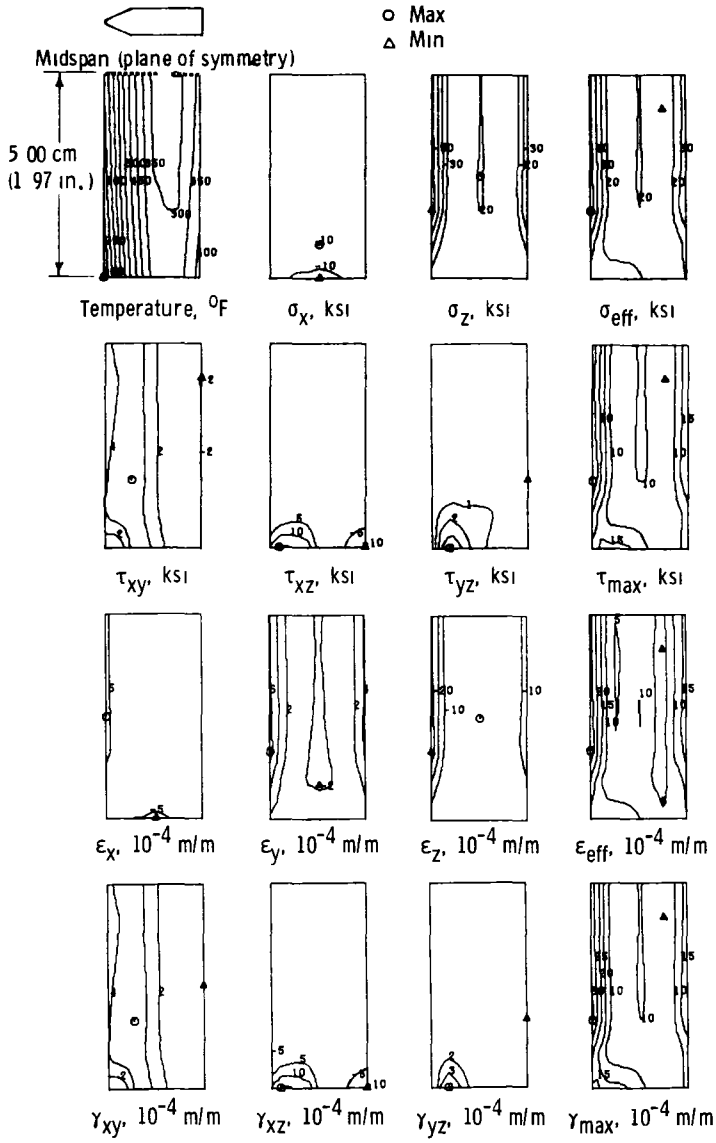

(d) 316 stainless steel alloy with the fluidized beds maintained at 960° and 21° C (1760° and 70° F) after 9 seconds immersion in the heating bed

Figure 6 - Continued

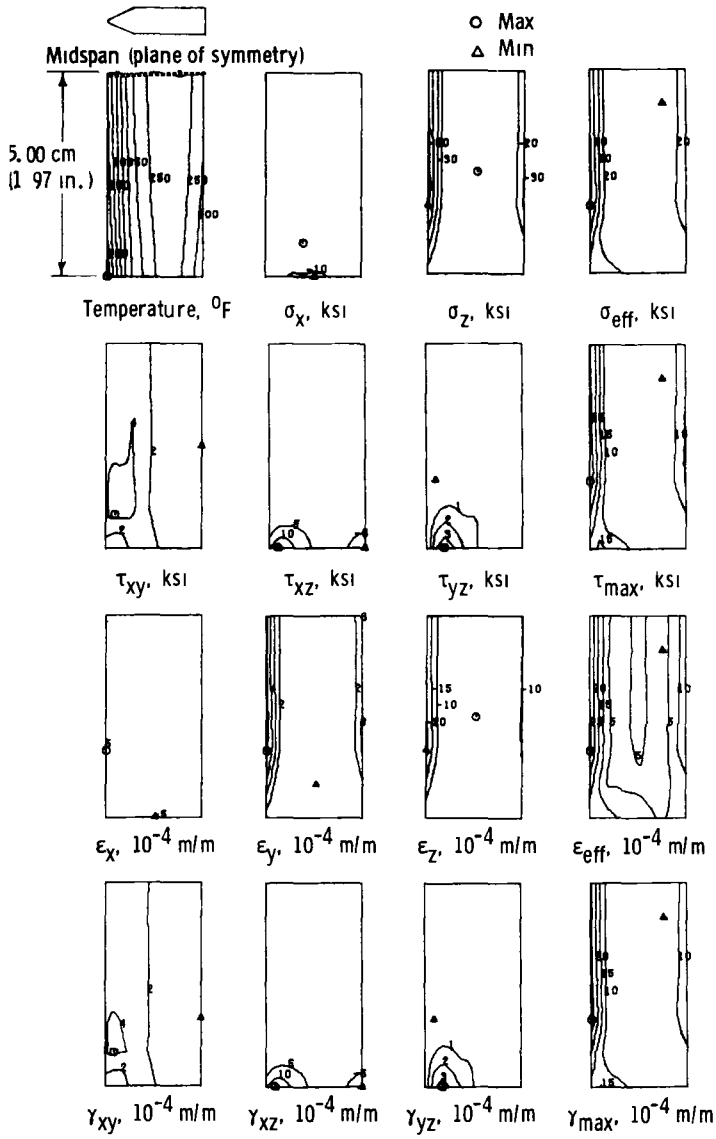

(e) A-286 alloy with the fluidized beds maintained at 740° and 21° C (1364° and 70° F) after 9 seconds immersion in the heating bed

Figure 6 - Continued

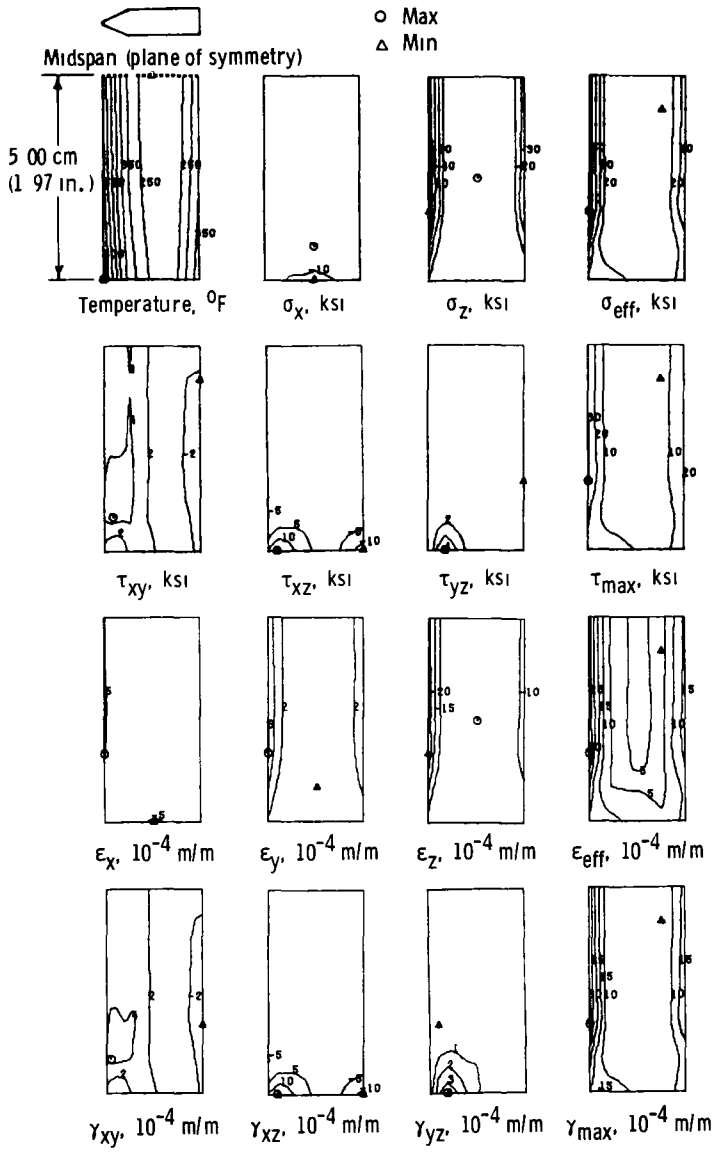

(f) A-286 alloy with the fluidized beds maintained at 850° and 21° C (1562° and 70° F) after 6 seconds immersion in the heating bed

Figure 6 - Continued

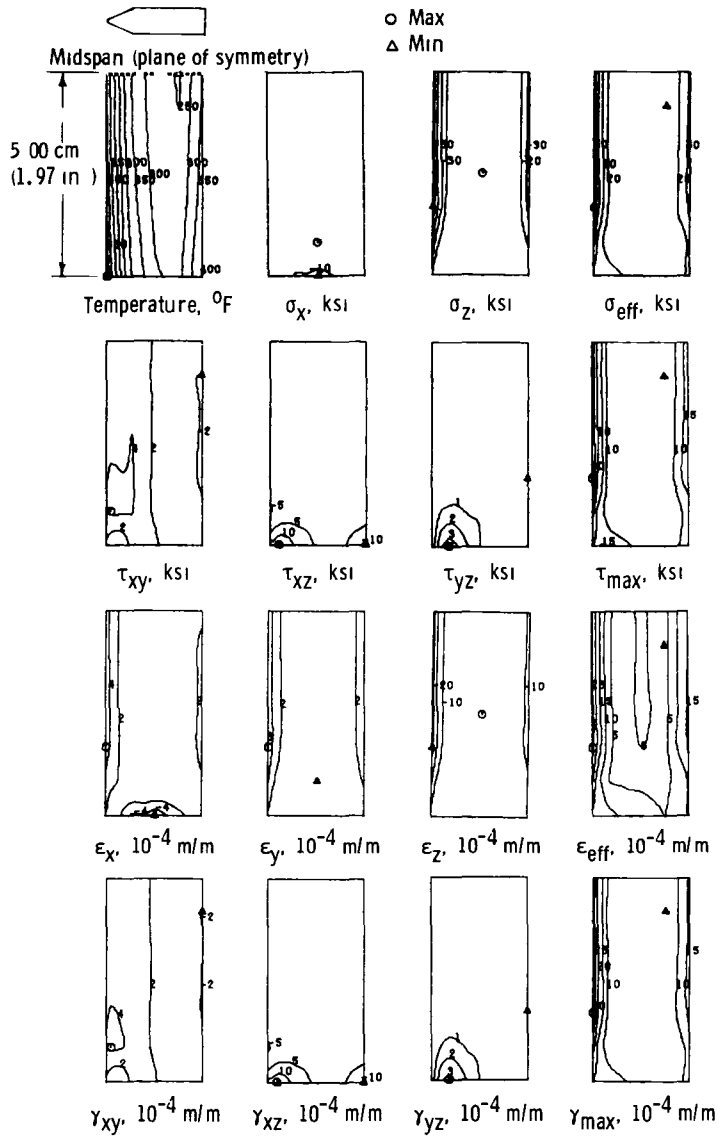

(g) A-286 alloy with the fluidized beds maintained at 960° and 21° C (1760° and 70° F) after 9 seconds immersion in the heating bed

Figure 6 - Concluded

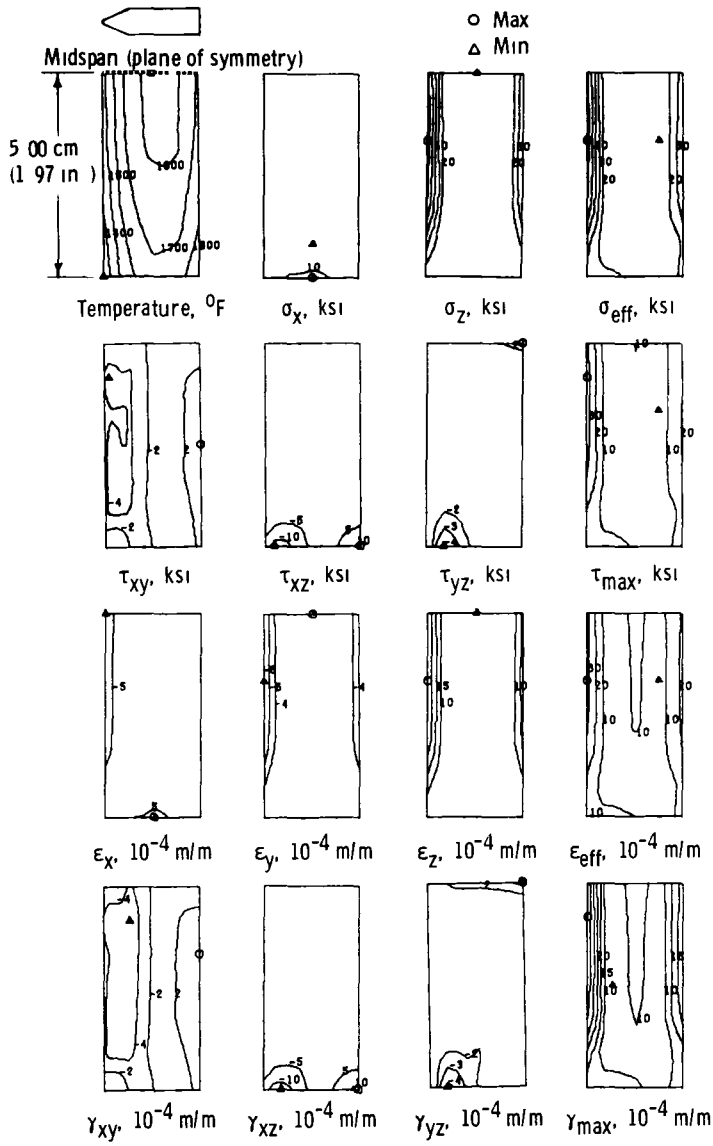

(a) NASA TAZ-8A alloy with fluidized beds maintained at 1088° and 316° C (1990° and 600° F) after 9 seconds immersion in the cooling bed

Figure 7 - Temperature, stress, and strain distribution of midchord at time of maximum leading edge longitudinal strain (F = 9/5 C + 32)(1 ksi = 6 895x10^6 N/m^2)

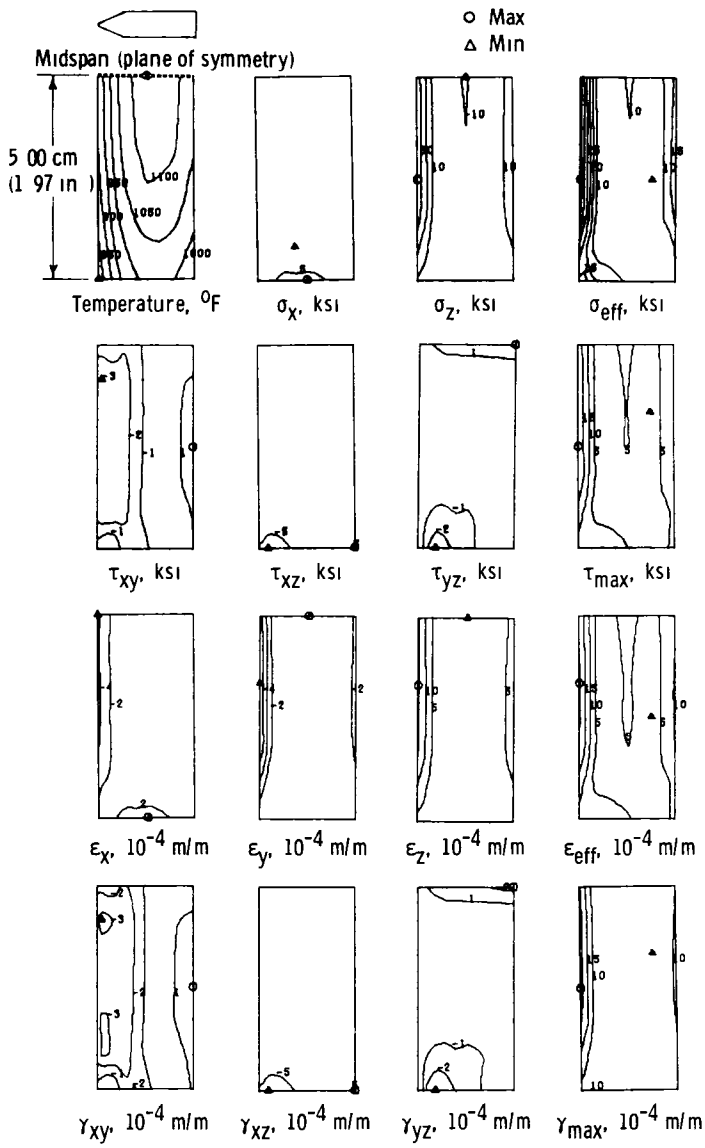

(b) 316 stainless steel alloy with the fluidized beds maintained at 740° and 21° C (1364° and 70° F) after 12 seconds immersion in the cooling bed

Figure 7 - Continued

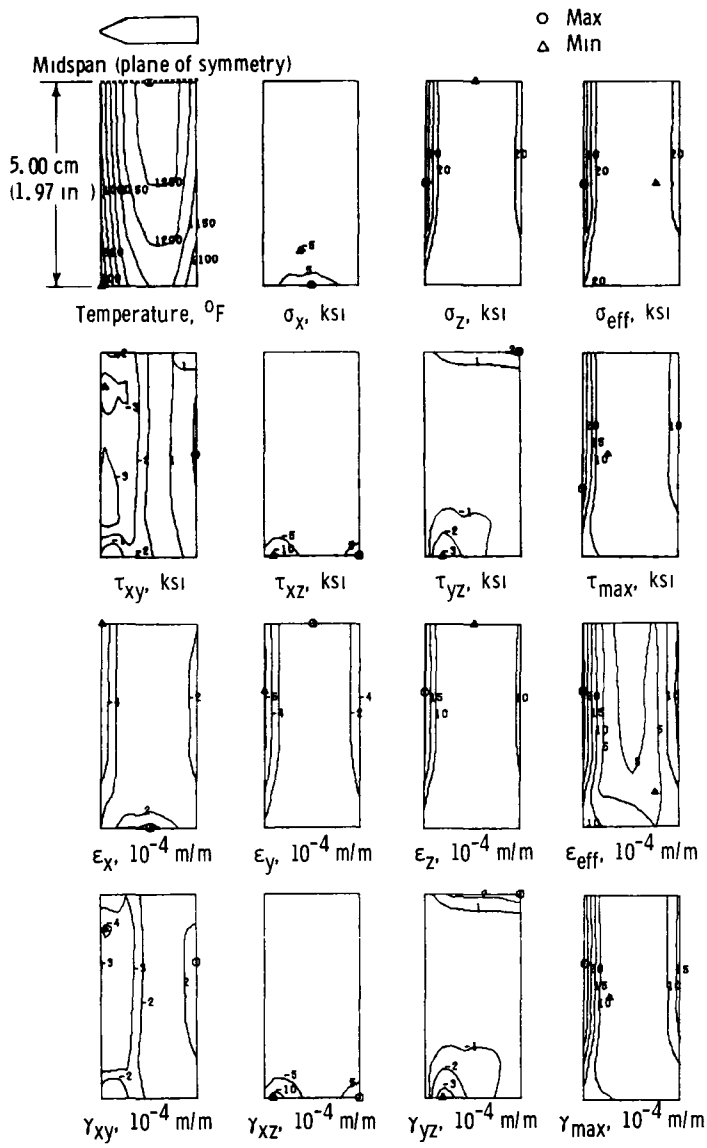

(c) 316 stainless steel alloy with the fluidized beds maintained at 850° and 21° C (1562° and 70° F) after 12 seconds immersion in the cooling bed.

Figure 7 - Continued

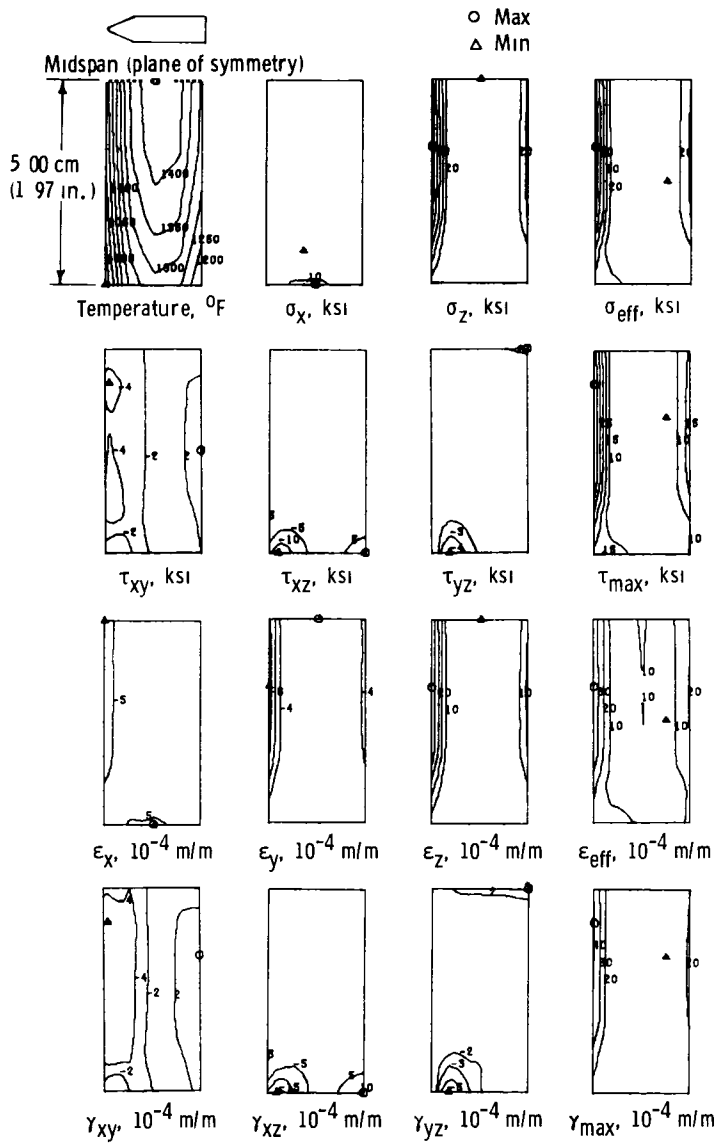

(d) 316 stainless steel alloy with the fluidized beds maintained at 960° and 21° C (1760° and 70° F) after 15 seconds immersion in the cooling bed

Figure 7 - Continued

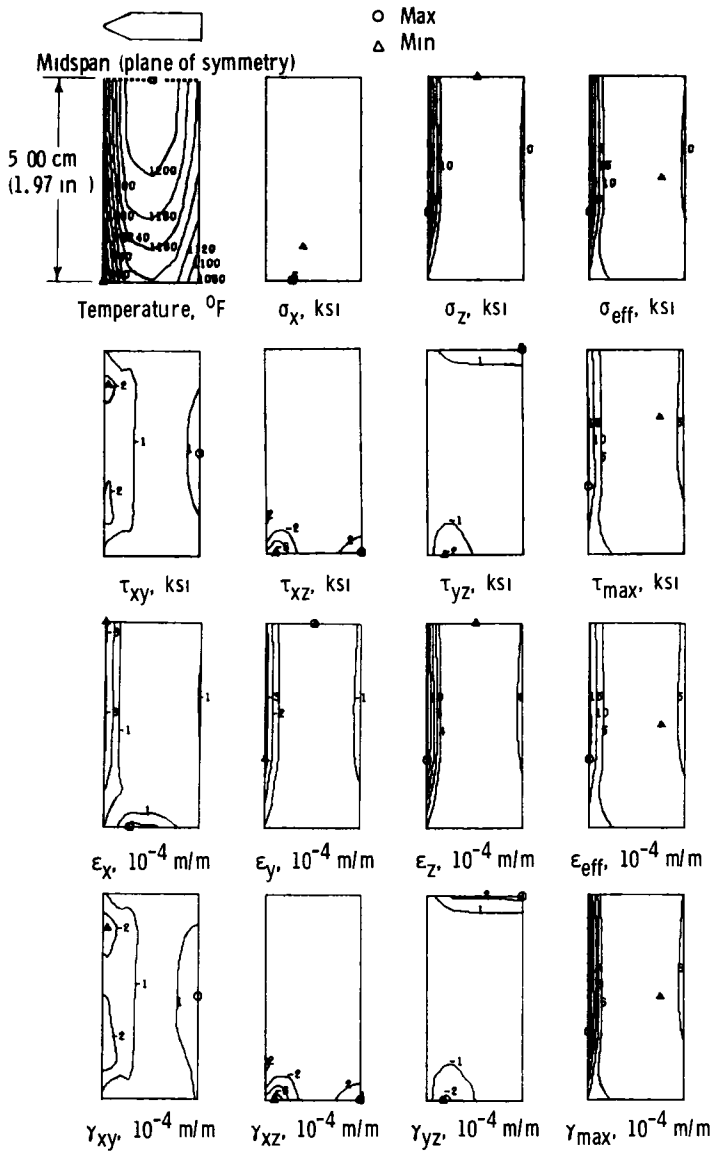

(e) A-286 alloy with the fluidized beds maintained at 740° and 21° C (1364° and 70° F) after 3 seconds immersion in the cooling bed

Figure 7 - Continued.

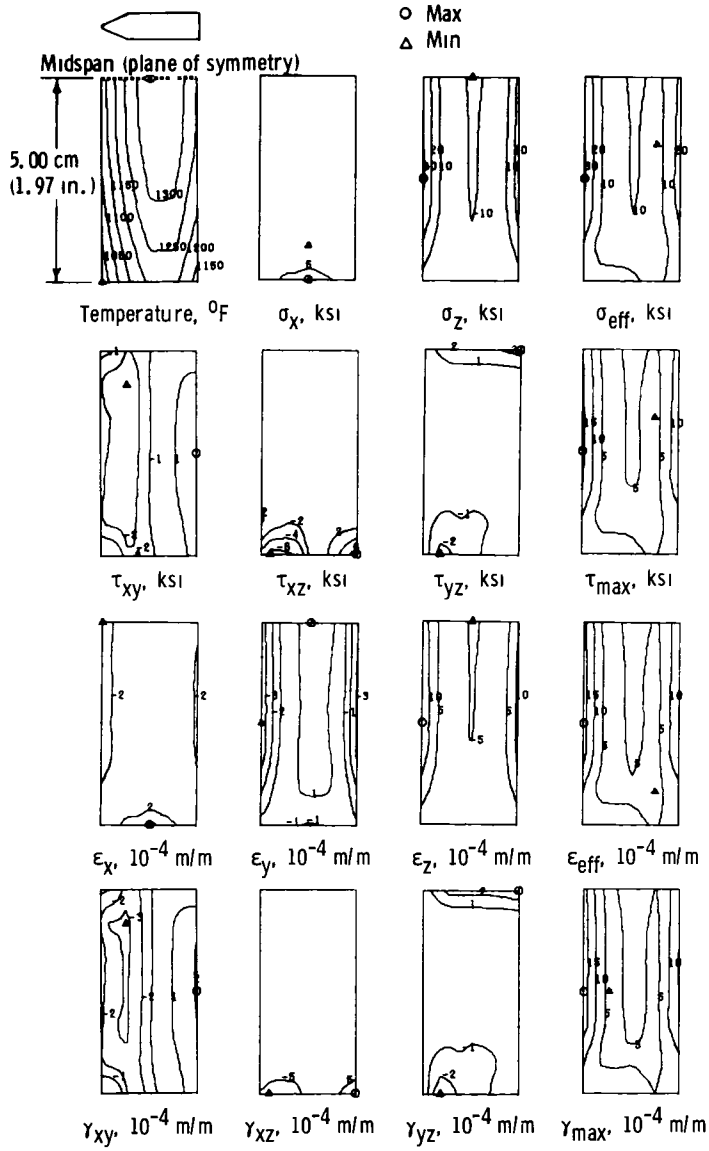

(f) A-286 alloy with the fluidized beds maintained at 850° and 21° C (1562° and 70° F) after 9 seconds immersion in the cooling bed

Figure 7 - Continued

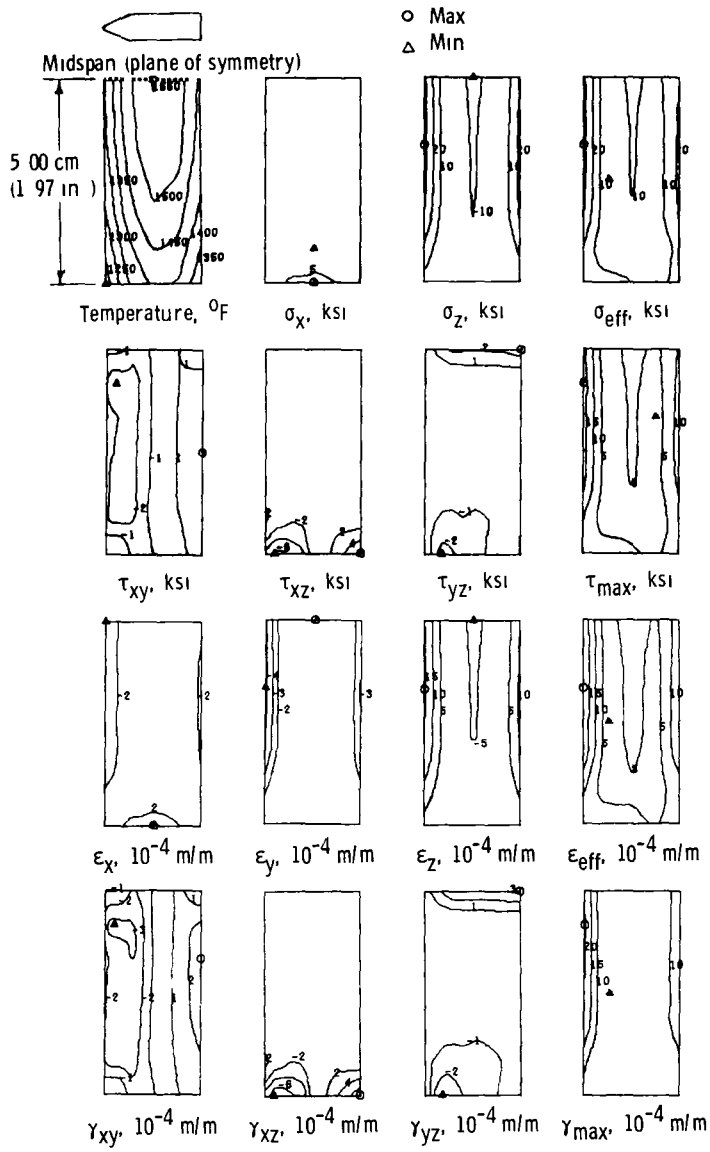

(g) A-286 alloy with the fluidized beds maintained at 960° and 21° C (1760° and 70° F) after 6 seconds immersion in the cooling bed

Figure 7 - Concluded

End of Document